#9、#19 ではクラスター分離が悪く、SNP タイピングに失敗していた。ここで、多型の見られなかった SNP#13 は解析から除外した。

ミスマッチ導入プローブの検討

40 検体を用いてマルチプレックス SNP タイピングを行った。ミスマッチを導入した 5'クエリープローブを用いると、SNP#6 と SNP#9 においてクラスター分離が改善され SNP タイピングに成功することが明らかとなった。この結果、ミスマッチ導入プローブを用いた際のタイピング成功率は 96.3%となることが分かった。

D.考察

DigiTag 法では、解析対象となる SNP の対立遺伝子型を DCNs へと変換してから解析を行う。物理化学的性質が一様となるように設計された DCNs を用いて解析を行うことにより、SNP タイピングを正確にかつ高い再現性で行えることが明らかとなった。また、エンコード反応に用いる 5'クエリープローブにミスマッチを導入することにより、より高い成功率で SNP タイピングを行えることが分かった。一方、クラスター分離の悪かった SNP#19 では、シグナル強度が弱く検出されたために解析が難しくなっている様子が見られた。これは、マルチプレックス PCR における増幅産物量が不十分であったことが原因であると考えられる。

DigiTag 法の特徴のひとつとして汎用性の高さが挙げられる。解析対象となる SNPs に対して自由に DCNs を割り当てられることから、エンコード反応以降は共通の素材および実験条件で解析を行うことができる。また、解析対象を SNPs ではなく cDNA とすることで遺伝子発現解析を行うことが可能であることもすでに確認している。これらの特徴は本手法がより安価な遺伝情報解析のプラットホームとなりうることを示している。

E.結論

DigiTag 法と名付けた新たなマルチプレックス SNP タイピング法を開発し、28 種の SNPs の同時タイピングを試みたところ、96%（26／27）という高い成功率が達成され、またシークエンシング結果との一致率も 100%と極めて有望な技術であることがわかった。今後、より一層簡便化したプロトコルを確立し、薬剤代謝や薬剤トランスポートに関わる遺伝子群の機能的多型をタイピングできるキット開発につなげる予定である。

F.健康危険情報

該当なし

G.研究発表

4. 論文発表

1) Nishida N, Tanabe T, Hashido K, Hirayasu K, Takasu M, Suyama A and Tokunaga K: DigiTag assay for multiplex SNP typing with high success rate. Anal. Biochem. 346(2): 281-288, 2005.

2) Bannai M, and Tokunaga K: Single nucleotide polymorphism typing using degenerate-oligonucleotide-primed PCR-amplified products. In: Whole Genome Amplification. (Ed. S. Hughes and R. Lasken) Scion Publishing Ltd.: 11-21, 2005.

2. 学会発表

1) 西田奈央、田邊哲也、金子善興、高須美和、陶山　明、徳永勝士：新規マルチプレックス SNP タイピング法の開発、日本人類遺伝学会第 50 回大会プログラム・抄録集、p133, 2005.9.20. 倉敷

2) Nishida N, Tanabe T, Takasu M, Kaneko Y, and Tokunaga K: A newly developed multiplex SNP typing method, DigiTag assay. The American Society of Human Genetics 55th Annual Meeting Abstracts p255, 2005.10.26ー28. Salt Lake City.

3) 西田奈央、田邊哲也、金子善興、高須美和、陶山　明、徳永勝士：DigiTag 法によるマルチプレックス SNP タイピング、第 28 回日本分子生物学会年会プログラム、p302、2005.12.9. 福岡

H.知的財産権の出願・登録状況

1. 特許出願

標的核酸を検出又は定量する方法（特願 2004-296784）

別紙４

研究成果の刊行に関する一覧表

書籍

著者氏名	論文タイトル名	書籍全体の編集者名	書　籍　名	出版社名	出版地	出版年	ページ
前田和哉, 杉山雄一	抗がん剤の効果・副作用に関連する薬剤代謝酵素・トランスポーターの遺伝子多型性	金倉 譲 編	臨床腫瘍内科学入門	永井書店	大阪	2005	130-137
前田和哉, 杉山雄一	解毒・排出系の遺伝子多型	松島綱治、酒井敏行、石川昌、稲寺秀邦 編	予防医学事典	朝倉書店	東京	2005	220-222
Bannai M, and Tokunaga K	Single nucleotide polymorphism typing using degenerate-oligonucleotide-primed PCR-amplified products	S. Hughes and R. Lasken	Whole Genome Amplification	Scion Publishing Ltd.	England	2005	11-21

雑誌

発表者氏名	論文タイトル名	発表誌名	巻号	ページ	出版年
Hirano, M., Maeda, K., Hayashi, H., Kusuhara, H. and Sugiyama, Y.	Bile salt export pump (BSEP/ABCB11) can transport a nonbile acid substrate, pravastatin	J Pharmacol Exp Ther	314	876-82	2005
Hirano, M., Maeda, K., Matsushima, S., Nozaki, Y., Kusuhara, H. and Sugiyama, Y.	Involvement of BCRP (ABCG2) in the biliary excretion of pitavastatin	Mol Pharmacol	68	800-7	2005
Hirono, S., Nakagome, I., Imai, R., Maeda, K., Kusuhara, H. and Sugiyama, Y.	Estimation of the three-dimensional pharmacophore of ligands for rat multidrug-resistance-associated protein 2 using ligand-based drug design techniques	Pharm Res	22	260-9	2005
Hirouchi, M., Suzuki, H. and Sugiyama, Y.	Treatment of Hyperbilirubinemia in Eisai Hyperbilirubinemic Rat by Transfecting Human MRP2/ABCC2 Gene	Pharm Res	22	661-6	2005

Matsushima, S., Maeda, K., Kondo, C., Hirano, M., Sasaki, M., Suzuki, H. and Sugiyama, Y.	Identification of the Hepatic Efflux Transporters of Organic Anions Using Double-Transfected Madin-Darby Canine Kidney II Cells Expressing Human Organic Anion-Transporting Polypeptide 1B1 (OATP1B1)/Multidrug Resistance-Associated Protein 2, OATP1B1/Multidrug Resistance 1, and OATP1B1/Breast Cancer Resistance Protein	J Pharmacol Exp Ther	314	1059-67	2005
Mita, S., Suzuki, H., Akita, H., Hayashi, H., Onuki, R., Hofmann, A. F. and Sugiyama, Y.	Vectorial transport of unconjugated and conjugated bile salts by monolayers of LLC-PK1 doubly transfected with human NTCP and BSEP or with rat Ntcp and Bsep	Am J Physiol Gastrointest Liver Physiol	290	G550-6	2006
Shimizu, M., Fuse, K., Okudaira, K., Nishigaki, R., Maeda, K., Kusuhara, H. and Sugiyama, Y.	Contribution of oatp (organic anion-transporting polypeptide) family transporters to the hepatic uptake of fexofenadine in humans	Drug Metab Dispos	33	1477-81	2005
Hayashi, H., Takada, T., Suzuki, H., Akita, H. and Sugiyama, Y.	Two common PFIC2 mutations are associated with the impaired membrane trafficking of BSEP/ABCB11	Hepatology	41	916-24	2005
Hayashi, H., Takada, T., Suzuki, H., Onuki, R., Hofmann, A. F. and Sugiyama, Y.	Transport by vesicles of glycine- and taurine-conjugated bile salts and taurolithocholate 3-sulfate: a comparison of human BSEP with rat Bsep	Biochim Biophys Acta	1738	54-62	2005
家入一郎	トランスポーターの遺伝子多型と臨床	臨床化学	34	5-10	2005
家入一郎	薬物トランスポーターと薬剤感受性(1)-薬物トランスポーター遺伝子多型の臨床的意義-	最新医学	60	1827-1832	2005
Nishida N, Tanabe T, Hashido K, Hirayasu K, Takasu M, Suyama A and Tokunaga K	DigiTag assay for multiplex SNP typing with high success rate	Anal Biochem	346	281-288	2005

IV. 研究成果の刊行物・別刷

0022-3565/05/3142-876–882$20.00
THE JOURNAL OF PHARMACOLOGY AND EXPERIMENTAL THERAPEUTICS
Copyright © 2005 by The American Society for Pharmacology and Experimental Therapeutics
JPET 314:876–882, 2005

Vol. 314, No. 2
84830/3044046
Printed in U.S.A.

Bile Salt Export Pump (BSEP/ABCB11) Can Transport a Nonbile Acid Substrate, Pravastatin

Masaru Hirano, Kazuya Maeda, Hisamitsu Hayashi, Hiroyuki Kusuhara, and Yuichi Sugiyama

Graduate School of Pharmaceutical Sciences, The University of Tokyo, Tokyo, Japan

Received February 11, 2005; accepted May 16, 2005

ABSTRACT

Pravastatin is a well known 3-hydroxy-3-methylglutaryl-CoA reductase inhibitor. Cumulative studies have shown that pravastatin is taken up into hepatocytes by the organic anion transporting polypeptide family transporters and excreted into the bile as an intact form by multidrug resistance-associated protein 2 (MRP2). It is generally accepted that the bile salt export pump (BSEP/ABCB11) mainly transports bile acids and plays an indispensable role in their biliary excretion. Interestingly, we found that BSEP could accept pravastatin as a substrate. Significant ATP-dependent uptake of pravastatin by human BSEP (hBSEP)- and rat BSEP (rBsep)-expressing membrane vesicles was observed, and the ratio of the uptake activity of pravastatin to that of taurocholic acid (TCA) by hBSEP was 3.3-fold higher than that by rBsep. The K_m value of pravastatin for hBSEP was 124 μM. A mutual inhibition study between TCA and pravastatin revealed that they competitively interact with hBSEP. Several statins inhibited the hBSEP- and rBsep-mediated uptake of TCA; however, the specific uptake of other statins (cerivastatin, fluvastatin, and pitavastatin) by hBSEP and rBSEP was not detected. The inhibitory effects of hydrophilic statins (pravastatin and rosuvastatin) on the uptake of TCA by BSEP were relatively lower than those of lipophilic statins. These data suggest that BSEP may be partly involved in the biliary excretion of pravastatin in both rats and humans.

The liver plays an important role in the excretion of xenobiotics, including many kinds of drugs. It has been reported that several kinds of transporters are expressed on both the sinusoidal and canalicular membrane in the liver to excrete drugs efficiently into bile (Kullak-Ublick et al., 2004). ABC transporters, which are driven by ATP hydrolysis, are expressed on the canalicular membrane and are responsible for the export of endogenous and xenobiotic compounds from the intracellular compartment. For example, multidrug resistance-associated protein 2 (MRP2/ABCC2) recognizes organic anions, such as glutathione- and glucuronide-conjugates, as substrates, whereas multidrug resistance 1 (MDR1/P-glycoprotein/ABCB1) preferentially accepts neutral/cationic hydrophobic compounds, and breast cancer resistance protein (BCRP/ABCG2) can also accept several kinds of anionic compounds, such as sulfate conjugates (Kullak-Ublick et al., 2004). Bile salt export pump (BSEP/ABCB11) is also expressed in the canalicular membrane. BSEP shares a high degree of sequence homology with MDR1 and was originally called the sister of P-glycoprotein (SPGP) (Gerloff et al., 1998; Lecureur et al., 2000). However, it has been found that BSEP does not show a broad substrate specificity compared with MDR1, and mainly recognizes bile acids (Madon et al., 2000; Noe et al., 2001, 2002; Byrne et al., 2002). In addition, mutations in the BSEP gene are associated with progressive familial intrahepatic cholestasis type II, and therefore BSEP plays an essential role in the biliary excretion of bile acids (Strautnieks et al., 1998). On the other hand, only a few nonbile acid substrates (vinblastine and some fluorescent substrates) have been reported to date (Lecureur et al., 2000; Wang et al., 2003a).

Pravastatin cannot easily penetrate the cell membrane due to its hydrophilicity, but it is selectively distributed to the liver (Komai et al., 1992). Considering that pravastatin is mainly excreted into bile without extensive metabolism, several transporters are thought to be important regulators of the pharmacokinetics of pravastatin. Pravastatin is taken up into hepatocytes by organic anion transporting polypeptide

This work was supported by Health and Labor Sciences Research grants from the Ministry of Health, Labor, and Welfare for the Research on Advanced Medical Technology and Grant-in-Aid for Young Scientists B 15790087 from the Ministry of Education, Culture, Sports, Science and Technology.
Article, publication date, and citation information can be found at http://jpet.aspetjournals.org.
doi:10.1124/jpet.105.084830.

ABBREVIATIONS: ABC, ATP-binding cassette; MRP/Mrp, multidrug resistance-associated protein; BSEP/bsep, bile salt export pump; OATP/Oatp, organic anion transporting polypeptide; EHBR, Eisai hyperbiliruminemic rat; SDR, Sprague-Dawley rat; CMV, canalicular membrane vesicle; E_1S, estrone-3-sulfate; TCA, taurocholic acid; MTX, methotrexate; hBSEP, human bile salt export pump; rBsep, rat bile salt export pump; GFP, green fluorescent protein; HEK, human embryonic kidney.

(OATP) 1B1 (OATP-C) in humans (Nakai et al., 2001) and several Oatp family transporters in rats (Yamazaki et al., 1993; Tokui et al., 1999), and it is excreted into bile in unchanged form, predominantly via Mrp2 in rats (Yamazaki et al., 1996). In particular, Yamazaki et al. (1997) reported that the biliary excretion clearance of pravastatin in Eisai hyperbilirubinemic rats (EHBR), which are Mrp2-deficient, was much lower than that in control Sprague-Dawley rats (SDR). Moreover, the ATP-dependent uptake of pravastatin in canalicular membrane vesicles (CMVs) prepared from EHBR was reduced compared with that in SDR (Yamazaki et al., 1997). From these results, it seems that Mrp2 is mainly responsible for the biliary excretion of pravastatin in rats. However, even in EHBR, the biliary excretion of pravastatin was partly maintained and the ATP-dependent uptake of pravastatin in CMVs prepared from EHBR was not abolished, suggesting that transporters other than MRP2 are also involved in the biliary excretion of pravastatin (Yamazaki et al., 1997), although they remain to be identified.

In a preliminary experiment, we found that pravastatin is a good substrate of human BSEP. In the present study, the transport properties of some statins were investigated using membrane vesicles expressing rat and human BSEP. We also observed the inhibitory effects of the statins on the uptake of TCA and clarified the relationship between the lipophilicity and inhibitory potency of the statins.

Materials and Methods

Materials. [^{3}H]Pravastatin (44.6 Ci/mmol) and [^{14}C]fluvastatin (45.7 mCi/mmol) were supplied by Sankyo Co., Ltd. (Tokyo, Japan) and Novartis (Basel, Switzerland), respectively. [^{3}H]Pitavastatin (16.0 Ci/mmol) and unlabeled 3-hydroxy-3-methylglutaryl-CoA reductase inhibitors (atorvastatin, cerivastatin, fluvastatin, pitavastatin, pravastatin, rosuvastatin, simvastatin acid, atorvastatin lactone, pitavastatin lactone, pravastatin lactone, and simvastatin) were donated by Kowa Co., Ltd. (Tokyo, Japan). [^{3}H]Estrone-3-sulfate (E_1S; 57.3 Ci/mmol) and [^{3}H]taurocholic acid (TCA; 3.50 Ci/mmol) were purchased from PerkinElmer Life and Analytical Sciences (Boston, MA). [^{3}H]Methotrexate (MTX; 29.0 Ci/mmol) was purchased from American Radiolabeled Chemicals (St. Louis, MO). [^{14}C]Temocaprilat was prepared by hydrolysis of [^{14}C]temocapril (5 N NaOH for 5 h) (Schwab et al., 1992), which was supplied by Sankyo Co., Ltd. The radiochemical purity of [^{14}C]temocaprilat was checked by thin layer chromatography (*n*-butanol/acetic acid/distilled water; 4:1:1) and confirmed to be more than 95%. Unlabeled E_1S, TCA, and MTX were purchased from Sigma-Aldrich (St. Louis, MO). All other chemicals were commercially available and of analytical grade.

Construction and Infection of Recombinant Adenovirus and Membrane Vesicle Preparation. The construction of recombinant adenovirus of human BSEP (hBSEP), rat BSEP (rBsep), and green fluorescent protein (GFP) has been described in detail previously (Hayashi et al., 2005). Membrane vesicles were prepared from hBSEP-, rBsep-, and GFP-transfected HEK293 cells according to the method described previously (Hayashi et al., 2005). HEK293 cells were cultured in Dulbecco's modified Eagle's medium (low glucose) (Invitrogen, Carlsbad, CA) supplemented with 10% fetal bovine serum, 100 U/ml penicillin, and 100 mg/ml streptomycin. For the preparation of the isolated membrane vesicles, HEK293 cells cultured in a 15-cm dish were infected by recombinant adenovirus of hBSEP or rBsep (25 multiplicity of infection). As a negative control, cells were infected with GFP (25 multiplicity of infection). Cells were harvested at 48 h after infection, and then the membrane vesicles were isolated from $1 \sim 2 \times 10^8$ cells using a standard method described in detail previously (Muller et al., 1994). Briefly, cells were diluted 40-fold with hypotonic buffer (1 mM Tris-HCl and 0.1 mM EDTA, pH 7.4, at 37°C) and stirred gently for 1 h on ice in the presence of 2 mM phenylmethylsulfonyl fluoride, 5 μg/ml leupeptin, 1 μg/ml pepstatin, and 5 μg/ml aprotinin. The cell lysate was centrifuged at 100,000*g* for 30 min at 4°C, and the pellet was suspended in 10 ml of ice-cold isotonic TS buffer (10 mM Tris-HCl and 250 mM sucrose, pH 7.4) and then homogenized with a Dounce B homogenizer (glass/glass, tight pestle, 30 strokes). The crude membrane fraction was layered on top of a 38% (w/v) sucrose solution in 5 mM Tris-HEPES, pH 7.4, at 4°C, and centrifuged in a Beckman SW41 rotor at 280,000*g* for 60 min at 4°C. The turbid layer at the interface was collected, diluted to 23 ml with TS buffer, and centrifuged at 100,000*g* for 30 min at 4°C. The resulting pellet was suspended in 400 μl of TS buffer. Vesicles were formed by passing the suspension 30 times through a 27-gauge needle using a syringe. The membrane vesicles were finally frozen in liquid nitrogen and stored at −80°C until use. Protein concentrations were determined by the Lowry method, and bovine serum albumin was used as a standard.

Transport Studies with Membrane Vesicles. The transport studies were performed using a rapid filtration technique (Hirohashi et al., 1999, 2000). Briefly, 15 μl of transport medium (10 mM Tris-HCl, 250 mM sucrose, and 10 mM $MgCl_2$, pH 7.4) containing radiolabeled compounds, with or without unlabeled substrates, was preincubated at 37°C for 3 min and then rapidly mixed with 5 μl of membrane vesicle suspension (5 μg of protein). The reaction mixture contained 5 mM ATP or AMP, along with the ATP-regenerating system (10 mM creatine phosphate and 100 μg/μl creatine phosphokinase). The transport reaction was terminated by the addition of 1 ml of ice-cold stop solution containing 10 mM Tris-HCl, 250 mM sucrose, and 0.1 M NaCl, pH 7.4; the reaction mixture was filtered through a 0.45-μm HA filter (Millipore Corporation, Billerica, MA) and then washed twice with 5 ml of stop solution. Filters with trapped membrane vesicles were mixed with scintillation cocktail (Clear-sol I; Nacalai Tesque, Tokyo, Japan), and the radioactivity retained on the filter was determined in a liquid scintillation counter (LS6000SE; Beckman Coulter Inc., Fullerton, CA).

Estimation of the Inhibitory Effect of the Statins on the BSEP-Mediated Transport of Bile Acids in Humans. To estimate the maximum inhibitory effect of the statins on the BSEP-mediated transport of bile acids in humans, the maximum unbound concentration at the liver inlet ($I_{in,max,u}$) was calculated from the following equation as described previously (Ito et al., 1998).

$$I_{in,max,u} = \left(C_{max,blood} + \frac{k_a \cdot D \cdot F_a}{Q_h} \right) \times f_{u,blood} \quad (1)$$

where $C_{max,blood}$ and $f_{u,blood}$ are the reported values of the maximum blood concentration of drug after oral administration of the clinical dose (D) and the protein unbound fraction in humans. In addition, k_a is set to a theoretically maximum absorption rate constant (6 h^{-1}) to avoid the false negative prediction of a drug interaction. F_a is the estimated fraction of the dose absorbed into and through the gastrointestinal membranes and calculated by the following equation:

$$F_a = \frac{F}{1 - \frac{CL_h}{Q_h}} \quad (2)$$

where CL_h is the reported hepatic clearance of drug, F is bioavailability, and Q_h is the hepatic blood flow rate (96.6 l/h). We calculated the ratio of AUC in the presence of inhibitors to that without inhibitors (R) from the following equation, assuming that the unbound concentration in liver (I) was 20-fold higher than that in blood, because statins were taken up and accumulated into hepatocytes by active transporters:

$$R = 1 + \frac{I}{K_i} \quad (3)$$

Kinetic Analyses. Ligand uptake was expressed as an uptake volume (microliters per milligram of protein), given as the amount of radioactivity associated with the membrane vesicles (dpm per milligram of protein) divided by the substrate concentration in the incubation medium (dpm per microliter). The ATP-dependent uptake of ligands via hBSEP or rBsep was calculated by subtracting the ligand uptake in the presence of AMP from that in the presence of ATP. Kinetic parameters were obtained using the following equation:

$$v = \frac{V_{max} \times S}{K_m + S} \quad (4)$$

where v is the uptake velocity of the substrate (picomoles per minute per milligram of protein), S is the substrate concentration in the medium (micromolar), K_m is the Michaelis constant (micromolar), and V_{max} is the maximum uptake rate (picomoles per minute per milligram of protein). Fitting was performed by the nonlinear least-squares method using a MULTI program (Yamaoka et al., 1981) and the Damping Gauss Newton Method algorithm was used for fitting. Inhibition constants (K_i) of a series of compounds could be calculated by the following equation, if the substrate concentration was low enough compared with its K_m value:

$$CL(+I) = \frac{CL}{(1 + I/K_i)} \quad (5)$$

where CL represents the uptake clearance in the absence of inhibitor, $CL(+I)$ represents the uptake clearance in the presence of inhibitor, and I represents the concentration of inhibitor. When fitting the data to determine the K_i value, the input data were weighed as the reciprocal of the observed values.

Statistical Analysis. Statistical differences were determined using one-way analysis of variance followed by Fisher's least significant difference method. Significant differences were considered at $P < 0.05$.

Results

ATP-Dependent Uptake of [^{3}H]Taurocholic Acid and [^{3}H]Pravastatin into Membrane Vesicles. The time profiles for the uptake of [^{3}H]TCA and [^{3}H]pravastatin by membrane vesicles obtained from recombinant adenovirus-infected HEK293 cells are shown in Fig. 1. The uptake of [^{3}H]TCA into membrane vesicles from hBSEP- and rBsep-transfected HEK293 cells, but not into those from GFP-transfected control cells, was markedly stimulated by ATP (Fig. 1, A and B). Significant ATP-dependent uptake of [^{3}H]pravastatin into hBSEP- and rBsep-expressing membrane vesicles was observed compared with that into control vesicles (Figs. 1, C and D, and 2A). The relative ATP-dependent uptake clearance of pravastatin to TCA by hBSEP was 3.3-fold higher than that by rBsep.

Uptake of Other Statins into Membrane Vesicles. Uptake of other statins into BSEP-expressing membrane vesicles was determined as well (Fig. 2). We were unable to find any significant ATP-dependent uptake of [^{3}H]cerivastatin, [^{14}C]fluvastatin, and [^{3}H]pitavastatin by hBSEP- and rBsep-expressing membrane vesicles compared with that by GFP-transfected vesicles, whereas both rBsep and hBSEP significantly recognized pravastatin as a substrate (Figs. 1 and 2). [^{3}H]E_1S (0.1 μM), [^{3}H]MTX (0.1 μM), and [^{14}C]temocaplirat (10 μM), which are relatively hydrophilic drugs, were also not accepted as substrates of either hBSEP or rBsep (data not shown).

Inhibitory Effects of Pravastatin and TCA on the hBSEP-Mediated Uptake. The concentration dependence of the hBSEP-mediated ATP-dependent uptake of pravastatin and TCA is shown in Fig. 3. The K_m values of pravastatin and TCA were 124 ± 13 and 4.64 ± 0.19 μM, respectively (Table 1). To characterize the mode of inhibition of TCA and pravastatin, we also performed a mutual inhibition study with TCA and pravastatin. The K_m and V_{max} values of TCA and pravastatin in the presence and absence of unlabeled pravastatin and TCA by hBSEP-expressing membrane vesicles are shown in Table 1. Judging from the shape of the Eadie-Hofstee plots in Fig. 3, their inhibition was competitive.

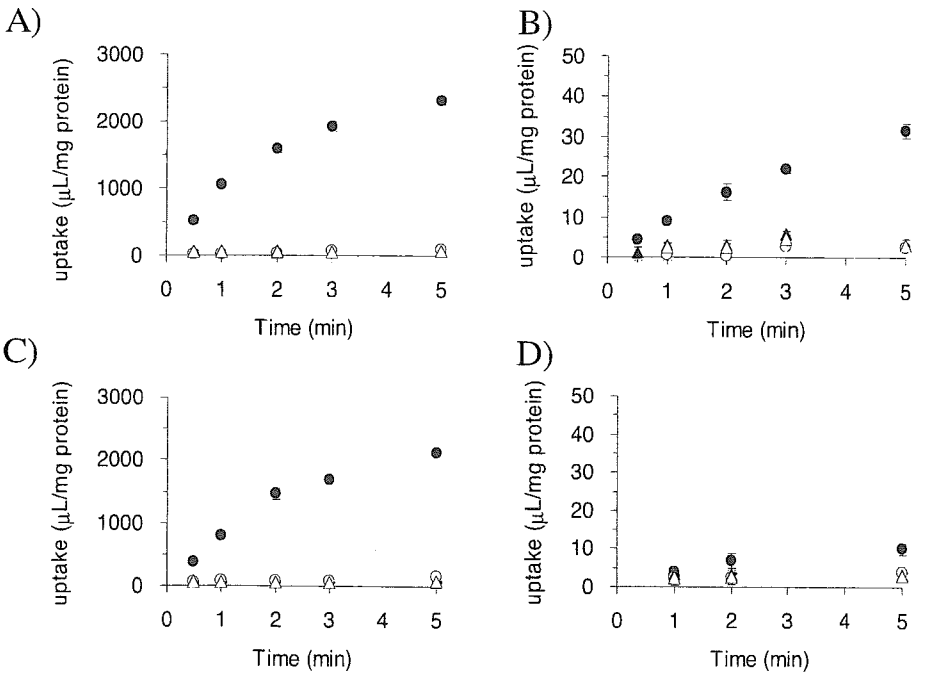

Fig. 1. Time profiles of the uptake of [^{3}H]TCA and [^{3}H]pravastatin by hBSEP and rBsep-expressing membrane vesicles. The uptake of 0.1 μM [^{3}H]TCA (A and B) and 0.1 μM [^{3}H]pravastatin (C and D) was observed at 37°C in the presence of 5 mM ATP (closed symbols) and 5 mM AMP (open symbols). The hBSEP- (A and C) and rBsep (B and D)-mediated uptake of [^{3}H]TCA or [^{3}H]pravastatin was determined. Circles and triangles represent the uptake in hBSEP- (or rBsep) and GFP-expressing membrane vesicles, respectively. Each point represents the mean ± S.E. (n = 3). Where vertical bars are not shown, the S.E. is within the limits of the symbols.

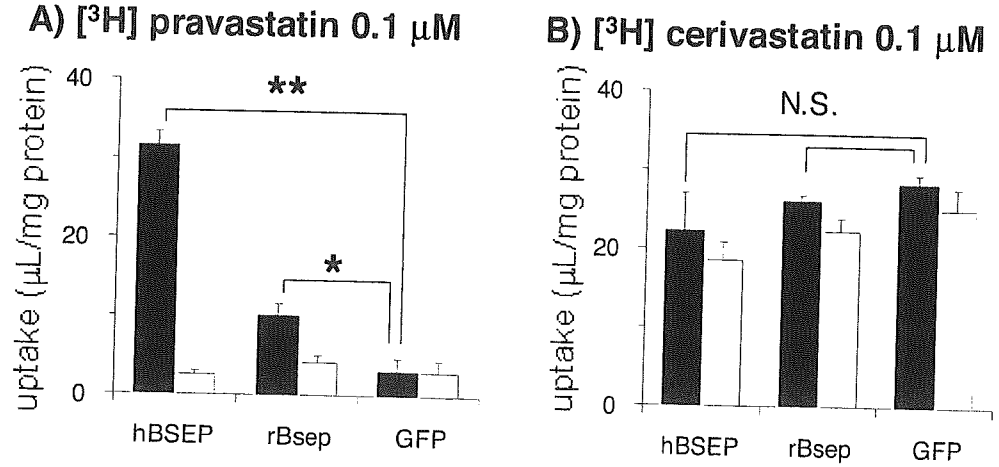

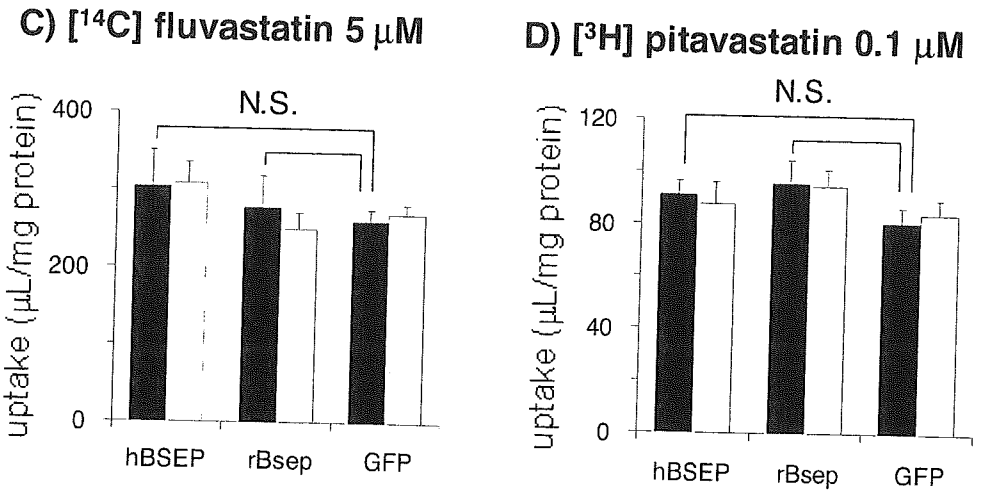

Fig. 2. Uptake of [^{3}H]pravastatin, [^{3}H]cerivastatin, [^{14}C]fluvastatin, and [^{3}H]pitavastatin by hBSEP- and rBsep-expressing membrane vesicles. The uptake of [^{3}H]pravastatin (A), [^{3}H]cerivastatin (B), [^{14}C]fluvastatin (C), and [^{3}H]pitavastatin (D) for 5 min was determined at 37°C in the presence of 5 mM ATP (closed symbols) and 5 mM AMP (open symbols). Each point represents the mean ± S.E. (n = 3). N.S., difference not significant compared with GFP-expressing control vesicles. *, $p < 0.05$; **, $p < 0.01$.

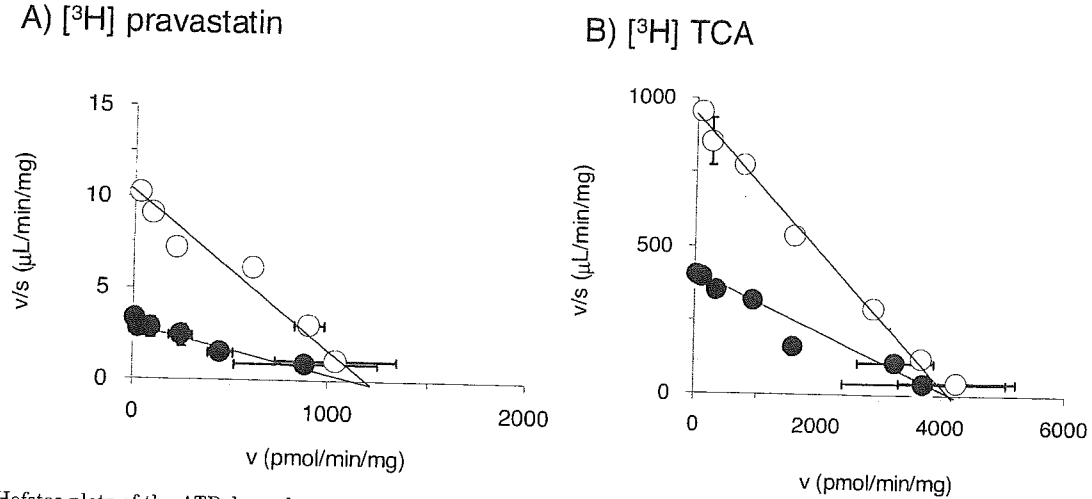

Fig. 3. Eadie-Hofstee plots of the ATP-dependent uptake of [^{3}H]pravastatin and [^{3}H]TCA in the presence and absence of unlabeled pravastatin and TCA by hBSEP-expressing membrane vesicles. The hBSEP-mediated uptake of [^{3}H]pravastatin (A) for 3 min and [^{3}H]TCA (B) for 2 min was measured in the presence (closed circles) and absence (open circles) of unlabeled TCA (3 μM) (A) and unlabeled pravastatin (250 μM) (B), respectively. Each point represents the mean ± S.E. (n = 3). The data were fitted to the Michaelis-Menten equation by nonlinear regression analysis as described under *Materials and Methods*, and each solid line represents the fitted curve.

Inhibitory Effects of the Statins on the ATP-Dependent Uptake of [^{3}H]TCA into hBSEP- and rBsep-Expressing Membrane Vesicles. We determined the inhibitory effects of the statins on the ATP-dependent uptake of [^{3}H]TCA by hBSEP- and rBsep-expressing membrane vesicles. All the statins (atorvastatin, cerivastatin, fluvastatin, pitavastatin, pravastatin, rosuvastatin, and simvastatin acid) that we tested were able to inhibit the ATP-dependent uptake of [^{3}H]TCA in a dose-dependent manner. The K_i values of the statins for hBSEP and rBsep are summarized in Table 2. On the other hand, the K_i value of TCA on the ATP-dependent uptake of pravastatin was 2.20 ± 0.52 μM (data not shown).

Comparison of K_i Values of the Statins for hBSEP with Those for rBsep. Comparing the K_i values of the

TABLE 1

K_m and V_{max} values of [^{3}H]pravastatin and [^{3}H]TCA in the presence and absence of unlabeled pravastatin and TCA by hBSEP-expressing membrane vesicles

The kinetic parameters were calculated from Fig. 3. The values are expressed as mean ± computer-calculated S.D.

Substrate	Inhibitor	K_m	V_{max}
		μM	*pmol/min/mg protein*
TCA		4.64 ± 0.19	4290 ± 120
	Pravastatin (250 μM)	9.91 ± 1.34	3880 ± 390
Pravastatin		124 ± 13	1220 ± 90
	TCA (3 μM)	366 ± 50	1110 ± 120

TABLE 2

Inhibitory effects of the statins on the ATP-dependent uptake of TCA by hBSEP- and rBsep-expressing membrane vesicles

The values are expressed as mean ± computer-calculated S.D. The log P values were estimated by Ishigami et al. (2001).

Statin	Log P	K_i Value for hBSEP	K_i Value for rBSEP
		μM	
Atorvastatin	1.5	9.12 ± 0.82	7.57 ± 1.17
Cerivastatin	2.3	11.4 ± 1.3	30.3 ± 4.1
Fluvastatin	1.8	30.2 ± 4.5	30.7 ± 3.1
Pitavastatin	1.5	25.6 ± 3.6	40.8 ± 4.8
Pravastatin	−0.47	163 ± 20	805 ± 97
Rosuvastatin	−0.30	120 ± 15	385 ± 59
Simvastatin acid	1.9	12.7 ± 1.4	30.0 ± 4.0
Atorvastatin lactone	4.2	13.7 ± 4.4	12.0 ± 5.3
Pitavastatin lactone	4.6[a]	59.9 ± 12.8	228 ± 48
Pravastatin lactone	2.4	37.6 ± 4.5	260 ± 35
Simvastatin (lactone)	4.4	23.1 ± 5.8	48.2 ± 10.4

[a] Calculated by ChemDraw version 7.0 (Chemical Drawing software; CambridgeSoft Corporation, Cambridge, MA).

statins for TCA transport by hBSEP with those by rBsep shown in Table 2, the inhibitory effect of the statins for hBSEP was slightly higher than that for rBsep. On the other hand, the rank order of the K_i values of the statins for hBSEP was almost the same as that for rBsep.

Discussion

In the present study, using membrane vesicles obtained from HEK293 cells infected with recombinant adenovirus of rat and human BSEP, we investigated the transport properties of pravastatin and other statins via BSEP in the biliary excretion process. We also examined the inhibitory effects of the statins on the uptake of TCA.

Significant ATP-dependent uptake of pravastatin was observed in both human and rat BSEP, but its relative uptake activity to TCA by hBSEP was 3.3 times higher than that by rBsep (Fig. 1). As shown in Fig. 3 and Table 1, the K_m values of pravastatin and TCA were 124 and 4.64 μM, which were almost consistent with the K_i values of pravastatin (163 μM; Table 2) and TCA (2.20 μM; data not shown), respectively. The mutual inhibition study between pravastatin and TCA was demonstrated that unlabeled TCA and pravastatin did not affect the V_{max} values in the ATP-dependent uptake of pravastatin and TCA, respectively (Fig. 3; Table 1). Judging from the shape of the Eadie-Hofstee plots, their inhibition might be competitive, suggesting that pravastatin and TCA might share the same binding site on hBSEP (Fig. 3). As shown in Fig. 2, the specific uptake of other statins, such as cerivastatin, fluvastatin and pitavastatin, was not detected in both hBSEP- and rBsep-expressing vesicles. In addition, at least, E_1S, temocaprilat and MTX are not accepted by BSEP (data not shown), implying that the substrate recognition of BSEP is relatively tightly controlled.

We previously demonstrated that the biliary excretion of pravastatin in EHBR was much lower than that in SDR and that ATP-dependent uptake of pravastatin by CMVs from EHBR was clearly reduced compared with that by CMVs from SDR. The K_m value (220 μM) of pravastatin uptake in CMVs from SDR was comparable with the K_i value (176 μM) for the uptake of 2,4-dinitrophenyl-*S*-glutathione, which is a typical substrate of Mrp2. These data suggest that Mrp2 is a major transporter in the biliary excretion of pravastatin in rats (Yamazaki et al., 1997). However, the biliary excretion as well as the ATP-dependent uptake in CMVs was slightly maintained even in EHBR, suggesting that transporters other than Mrp2 are also involved in the biliary excretion of pravastatin in rats (Adachi et al., 1996; Yamazaki et al., 1997). The K_m value of the ATP-dependent uptake of pravastatin in CMVs prepared from EHBR was 1050 μM (Adachi et al., 1996). In the present study, the ATP-dependent uptake of pravastatin into rBsep-expressing membrane vesicles was too low to determine the kinetic parameters. However, the K_i value of pravastatin for rBsep (805 μM) was comparable with the K_m value determined by CMVs from EHBR, and this does not conflict with our hypothesis that rBsep may be partly involved in the biliary excretion of pravastatin. In humans, the transcellular vectorial transport of pravastatin was clearly observed in MDCKII cells expressing OATP1B1 and MRP2 (Sasaki et al., 2002), whereas that of MDR1 and BCRP was relatively small (Matsushima et al., 2005). Although MRP2 is generally thought to be the main transporter for the biliary excretion of pravastatin, it is possible that BSEP is one of the candidates responsible for the remaining portion of its biliary excretion. Taking greater uptake activity of pravastatin by hBSEP into consideration, it is possible that the contribution of BSEP to the biliary excretion may become greater in humans than in rats. The relative contribution of BSEP to the biliary excretion of pravastatin will need to be clarified by using Bsep-knockout mice or by comparing the inhibitory effects of TCA on the biliary excretion of pravasta-

TABLE 3

Estimation of the inhibitory effect of the statins on BSEP-mediated transport of TCA in humans

The detailed method for calculation of these parameters is described under *Materials and Methods*. $C_{max,u,blood}$ ($=C_{max,blood} \times f_{u,blood}$) represents the reported values of the maximum unbound blood concentration, and $I_{in,max,u}$ represents the estimated maximum unbound concentration at the inlet to the liver. Simvastatin was administered as a lactone form. $C_{max,u,blood}$ was cited from other articles: simvastatin (Lilja et al., 1998); atorvastatin and pravastatin (Lilja et al., 1999); cerivastatin (Muck, 2000); pitavastatin (Fujino et al., 1998); and fluvastatin (Lennernas and Fager, 1997).

Statin	Atorvastatin	Cerivastatin	Fluvastatin	Pitavastatin	Pravastatin	Simvastatin
$C_{max,u,blood}$ (nM)	0.454	0.0696	4.18	1.67	58.6	0.444
$I_{in,max,u}$ (nM)	14.8	0.601	27.9	10.2	2294	104
Free concentration in liver (I) (μM)	0.295	0.0120	0.557	0.204	45.9	2.08
$1 + I/K_i$	1.03	1.00	1.02	1.01	1.28	1.16

tin between SDR and EHBR. In addition, when the expression or function of MRP2 is reduced by disease, genetic polymorphisms, and drug-drug interactions, BSEP may help excrete pravastatin into the bile, although the relative contribution of MRP2 and BSEP to the overall efflux of pravastatin remains to be determined in humans.

To investigate the affinities for BSEP among the statins, inhibitory effects of the statins were examined for the uptake of TCA by rBsep and hBSEP. The inhibition potency exhibited about a 100-fold difference among the statins. The rank order of the K_i values of the statins for hBSEP was almost the same as that for rBsep. In addition, the inhibitory effects of the acid forms of statins tended to be dependent on the lipophilicity of the drugs in both rBsep and hBSEP. The K_i values of hydrophilic acid forms of statins (pravastatin and rosuvastatin) for rBsep were larger than those for hBSEP, whereas those of lipophilic acid forms of statins were relatively similar (Table 2), which can partly explain why the relative uptake activity of pravastatin to TCA by rBsep was lower than that by hBSEP (Fig. 1). Regarding the lactone forms of statins, K_i value of the lactone forms except pravastatin for human and rat BSEP was slightly higher than that of the corresponding acid forms. Although the log P values of the lactone forms of statins are larger than those of acids forms, the K_i values of lactone forms were not different from those of lipophilic acid forms of statins, suggesting that the inhibition potency of acid and lactone forms of statins was not simply determined only by their lipophilicity.

Although only pravastatin was transported by BSEP, the K_i value of pravastatin was the highest among the statins. It is not surprising that the substrate for a transporter showed higher K_i value compared with nonsubstrate. For MRP2, the K_i values of vincristine and etoposide (802 and 756 μM, respectively) for the uptake of vinblastine were much higher than that of cyclosporine A (8.11 μM) (Tang et al., 2002). On the other hand, MRP2 could accept vincristine and etoposide (Chen et al., 1999; Guo et al., 2002), whereas there was no evidence that cyclosporine A was a substrate of MRP2.

In terms of inhibition of BSEP, a previous report has been indicated that many lipophilic drugs are inhibitors of BSEP such as tamoxifen, valinomycin, reserpine, rifamycin SV, cyclosporine A, troglitazone, and paclitaxel (Wang et al., 2003). Cyclosporine A and troglitazone, which are among the most potent known BSEP inhibitors, cause drug-induced cholestasis not only in rats but also in humans (Cadranel et al., 1992; Gitlin et al., 1998; Funk et al., 2001). It has been also reported that several kinds of the statins induce cholestasis in clinical situations (Ballare et al., 1991; Jimenez-Alonso et al., 1999; Batey and Harvey, 2002). So, to determine whether the inhibition of BSEP-mediated transport of bile acids by statins is clinically relevant, we calculated the maximum unbound concentration at the inlet to the liver using a method established in our laboratory to avoid the false negative prediction of drug-drug interactions (Ito et al., 1998). As shown in Table 3, even if the unbound concentration of the statins in the liver is 20-fold higher than that in plasma because uptake transporters can concentrate the statins efficiently into hepatocytes, the unbound concentration in liver is much lower than the K_i values for BSEP-mediated transport estimated in the present study. Therefore, although statins can inhibit BSEP-mediated transport in in vitro experiments, inhibition of BSEP-mediated transport by statins should not have a significant impact on drug interactions and statin-induced cholestasis in clinical situations.

So far, it has been reported that vinblastine and some fluorescent compounds (calcein-AM, bodipy, and dihydrofluoroscein) are accepted as substrates except for bile acids (Lecureur et al., 2000; Wang et al., 2003). In the present study, we also found that BSEP recognizes the nonbile acid pravastatin as a substrate and might be involved in the biliary excretion of pravastatin together with MRP2.

Acknowledgments

We thank Dr. Hidetaka Akita (Hokkaido University, Sapporo, Japan) and Sachiko Mita for cloning and construction of recombinant adenovirus of rBsep; Sankyo Co., Ltd. for providing labeled pravastatin and temocapril; Novartis for providing labeled fluvastatin; and Kowa Co., Ltd. for providing labeled pitavastatin and unlabeled statins.

References

Adachi Y, Okuyama Y, Miya H, Matsusita H, Kitano M, Kamisako T, and Yamamoto T (1996) Pravastatin transport across the hepatocyte canalicular membrane requires both ATP and a transmembrane pH gradient. *J Gastroenterol Hepatol* **11**:580–585.

Ballare M, Campanini M, Catania E, Bordin G, Zaccala G, and Monteverde A (1991) Acute cholestatic hepatitis during simvastatin administration. *Recenti Prog Med* **82**:233–235.

Batey RG and Harvey M (2002) Cholestasis associated with the use of pravastatin sodium. *Med J Aust* **176**:561.

Byrne JA, Strautnieks SS, Mieli-Vergani G, Higgins CF, Linton KJ, and Thompson RJ (2002) The human bile salt export pump: characterization of substrate specificity and identification of inhibitors. *Gastroenterology* **123**:1649–1658.

Cadranel JF, Erlinger S, Desruenne M, Luciani J, Lunel F, Grippon P, Cabrol A, and Opolon P (1992) Chronic administration of cyclosporin A induces a decrease in hepatic excretory function in man. *Dig Dis Sci* **37**:1473–1476.

Chen ZS, Kawabe T, Ono M, Aoki S, Sumizawa T, Furukawa T, Uchiumi T, Wada M, Kuwano M, and Akiyama SI (1999) Effect of multidrug resistance-reversing agents on transporting activity of human canalicular multispecific organic anion transporter. *Mol Pharmacol* **56**:1219–1228.

Fujino H, Kojima J, Yamada Y, Kanda H, and Kimata H (1998) Studies on the metabolic fate of NK-104, a new inhibitor of HMG-CoA reductase (4): interspecies variation in laboratory animals and humans. *Xenobio Metab Dispos* **14**:79–91.

Funk C, Pantze M, Jehle L, Ponelle C, Scheuermann G, Lazendic M, and Gasser R (2001) Troglitazone-induced intrahepatic cholestasis by an interference with the hepatobiliary export of bile acids in male and female rats. Correlation with the gender difference in troglitazone sulfate formation and the inhibition of the canalicular bile salt export pump (Bsep) by troglitazone and troglitazone sulfate. *Toxicology* **167**:83–98.

Gerloff T, Stieger B, Hagenbuch B, Madon J, Landmann L, Roth J, Hofmann AF, and Meier PJ (1998) The sister of P-glycoprotein represents the canalicular bile salt export pump of mammalian liver. *J Biol Chem* **273**:10046–10050.

Gitlin N, Julie NL, Spurr CL, Lim KN, and Juarbe HM (1998) Two cases of severe clinical and histologic hepatotoxicity associated with troglitazone. *Ann Intern Med* **129:**36–38.

Guo A, Marinaro W, Hu P, and Sinko PJ (2002) Delineating the contribution of secretory transporters in the efflux of etoposide using Madin-Darby canine kidney (MDCK) cells overexpressing P-glycoprotein (Pgp), multidrug resistance-associated protein (MRP1) and canalicular multispecific organic anion transporter (cMOAT). *Drug Metab Dispos* **30:**457–463.

Hayashi H, Takada T, Akita H, Suzuki H, and Sugiyama Y (2005) Two common PFIC2 mutations are associated with the impaired membrane trafficking of BSEP/ABCB11. *Hepatology* **41:**916–924.

Hirohashi T, Suzuki H, Chu XY, Tamai I, Tsuji A, and Sugiyama Y (2000) Function and expression of multidrug resistance-associated protein family in human colon adenocarcinoma cells (Caco-2). *J Pharmacol Exp Ther* **292:**265–270.

Hirohashi T, Suzuki H, and Sugiyama Y (1999) Characterization of the transport properties of cloned rat multidrug resistance-associated protein 3 (MRP3). *J Biol Chem* **274:**15181–15185.

Ishigami M, Honda T, Takasaki W, Ikeda T, Komai T, Ito K, and Sugiyama Y (2001) A comparison of the effects of 3-hydroxy-3-methylglutaryl-coenzyme a (HMG-CoA) reductase inhibitors on the CYP3A4-dependent oxidation of mexazolam in vitro. *Drug Metab Dispos* **29:**282–288.

Ito K, Iwatsubo T, Kanamitsu S, Ueda K, Suzuki H, and Sugiyama Y (1998) Prediction of pharmacokinetic alterations caused by drug-drug interactions: metabolic interaction in the liver. *Pharmacol Rev* **50:**387–412.

Jimenez-Alonso J, Osorio JM, Gutierrez-Cabello F, Lopez de la Osa A, Leon L, and Mediavilla Garcia JD (1999) Atorvastatin-induced cholestatic hepatitis in a young woman with systemic lupus erythematosus. Grupo Lupus Virgen de las Nieves. *Arch Intern Med* **159:**1811–1812.

Komai T, Kawai K, Tokui T, Tokui Y, Kuroiwa C, Shigehara E, and Tanaka M (1992) Disposition and metabolism of pravastatin sodium in rats, dogs and monkeys. *Eur J Drug Metab Pharmacokinet* **17:**103–113.

Kullak-Ublick GA, Stieger B, and Meier PJ (2004) Enterohepatic bile salt transporters in normal physiology and liver disease. *Gastroenterology* **126:**322–342.

Lecureur V, Sun D, Hargrove P, Schuetz EG, Kim RB, Lan LB, and Schuetz JD (2000) Cloning and expression of murine sister of P-glycoprotein reveals a more discriminating transporter than MDR1/P-glycoprotein. *Mol Pharmacol* **57:**24–35.

Lennernas H and Fager G (1997) Pharmacodynamics and pharmacokinetics of the HMG-CoA reductase inhibitors. Similarities and differences. *Clin Pharmacokinet* **32:**403–425.

Lilja JJ, Kivisto KT, and Neuvonen PJ (1998) Grapefruit juice-simvastatin interaction: effect on serum concentrations of simvastatin, simvastatin acid, and HMG-CoA reductase inhibitors. *Clin Pharmacol Ther* **64:**477–483.

Lilja JJ, Kivisto KT, and Neuvonen PJ (1999) Grapefruit juice increases serum concentrations of atorvastatin and has no effect on pravastatin. *Clin Pharmacol Ther* **66:**118–127.

Madon J, Hagenbuch B, Landmann L, Meier PJ, and Stieger B (2000) Transport function and hepatocellular localization of mrp6 in rat liver. *Mol Pharmacol* **57:**634–641.

Matsushima S, Maeda K, Kondo C, Hirano M, Sasaki M, Suzuki H, and Sugiyama Y (2005) Identification of the hepatic efflux transporters of organic anions using double transfected Madin-Darby Canine Kidney II cells expressing human organic anion transporting polypeptide 1B1 (OATP1B1)/multidrug resistance-associated protein 2, OATP1B1/multidrug resistance 1, and OATP1B1/breast cancer resistance protein. *J Pharmacol Exp Ther*, in press.

Muck W (2000) Clinical pharmacokinetics of cerivastatin. *Clin Pharmacokinet* **39:** 99–116.

Muller M, Meijer C, Zaman GJ, Borst P, Scheper RJ, Mulder NH, de Vries EG, and Jansen PL (1994) Overexpression of the gene encoding the multidrug resistance-associated protein results in increased ATP-dependent glutathione S-conjugate transport. *Proc Natl Acad Sci USA* **91:**13033–13037.

Nakai D, Nakagomi R, Furuta Y, Tokui T, Abe T, Ikeda T, and Nishimura K (2001) Human liver-specific organic anion transporter, LST-1, mediates uptake of pravastatin by human hepatocytes. *J Pharmacol Exp Ther* **297:**861–867.

Noe J, Hagenbuch B, Meier PJ, and St-Pierre MV (2001) Characterization of the mouse bile salt export pump overexpressed in the baculovirus system. *Hepatology* **33:**1223–1231.

Noe J, Stieger B, and Meier PJ (2002) Functional expression of the canalicular bile salt export pump of human liver. *Gastroenterology* **123:**1659–1666.

Sasaki M, Suzuki H, Ito K, Abe T, and Sugiyama Y (2002) Transcellular transport of organic anions across a double-transfected Madin-Darby canine kidney II cell monolayer expressing both human organic anion-transporting polypeptide (OATP2/SLC21A6) and multidrug resistance-associated protein 2 (MRP2/ABCC2). *J Biol Chem* **277:**6497–6503.

Schwab AJ, de Lannoy IA, Goresky CA, Poon K, and Pang KS (1992) Enalaprilat handling by the kidney: barrier-limited cell entry. *Am J Physiol* **263:**F858–F869.

Strautnieks SS, Bull LN, Knisely AS, Kocoshis SA, Dahl N, Arnell H, Sokal E, Dahan K, Childs S, Ling V, et al. (1998) A gene encoding a liver-specific ABC transporter is mutated in progressive familial intrahepatic cholestasis. *Nat Genet* **20:**233–238.

Tang F, Horie K, and Borchardt RT (2002) Are MDCK cells transfected with the human MRP2 gene a good model of the human intestinal mucosa? *Pharm Res* **19:**773–779.

Tokui T, Nakai D, Nakagomi R, Yawo H, Abe T, and Sugiyama Y (1999) Pravastatin, an HMG-CoA reductase inhibitor, is transported by rat organic anion transporting polypeptide, oatp2. *Pharm Res* **16:**904–908.

Wang EJ, Casciano CN, Clement RP, and Johnson WW (2003) Fluorescent substrates of sister-P-glycoprotein (BSEP) evaluated as markers of active transport and inhibition: evidence for contingent unequal binding sites. *Pharm Res* **20:**537–544.

Yamaoka K, Tanigawara Y, Nakagawa T, and Uno T (1981) A pharmacokinetic analysis program (multi) for microcomputer. *J Pharmacobio-Dyn* **4:**879–885.

Yamazaki M, Akiyama S, Ni'inuma K, Nishigaki R, and Sugiyama Y (1997) Biliary excretion of pravastatin in rats: contribution of the excretion pathway mediated by canalicular multispecific organic anion transporter. *Drug Metab Dispos* **25:**1123–1129.

Yamazaki M, Kobayashi K, and Sugiyama Y (1996) Primary active transport of pravastatin across the liver canalicular membrane in normal and mutant Eisai hyperbilirubinemic rats. *Biopharm Drug Dispos* **17:**607–621.

Yamazaki M, Suzuki H, Hanano M, Tokui T, Komai T, and Sugiyama Y (1993) Na(+)-independent multispecific anion transporter mediates active transport of pravastatin into rat liver. *Am J Physiol* **264:**G36–G44.

Address correspondence to: Dr. Yuichi Sugiyama, Department of Molecular Pharmacokinetics, Graduate School of Pharmaceutical Sciences, The University of Tokyo, 7-3-1 Hongo, Bunkyo-ku, Tokyo, 113-0033 Japan. E-mail: sugiyama@mol.f.u-tokyo.ac.jp

0026-895X/05/6803-800–807$20.00
MOLECULAR PHARMACOLOGY
Vol. 68, No. 3
14019/3048547

Mol Pharmacol 68:800–807, 2005
Printed in U.S.A.

Involvement of BCRP (ABCG2) in the Biliary Excretion of Pitavastatin

Masaru Hirano, Kazuya Maeda, Soichiro Matsushima, Yoshitane Nozaki, Hiroyuki Kusuhara, and Yuichi Sugiyama

Graduate School of Pharmaceutical Sciences, The University of Tokyo, Tokyo, Japan

Received April 20, 2005; accepted June 13, 2005

ABSTRACT

Pitavastatin, a novel potent 3-hydroxymethylglutaryl coenzyme A reductase inhibitor, is distributed selectively to the liver and excreted into bile in unchanged form in rats. We reported previously that the hepatic uptake is mainly mediated by organic anion transporting polypeptide (OATP) 1B1, whereas the biliary excretion mechanism remains to be clarified. In the present study, we investigated the role of breast cancer resistance protein (BCRP) in the biliary excretion of pitavastatin. The ATP-dependent uptake of pitavastatin by human and mouse BCRP-expressing membrane vesicles was significantly higher compared with that by control vesicles with K_m values of 5.73 and 4.77 μM, respectively. The biliary excretion clearance of pitavastatin in Bcrp1(−/−) mice was decreased to one-tenth of that in control mice. The biliary excretion of pitavastatin was unchanged between control and Eisai hyperbilirubinemic rats, indicating a minor contribution of multidrug resistance-associated protein (Mrp) 2. This observation differs radically from that for a more hydrophilic statin, pravastatin, of which biliary excretion is largely mediated by Mrp2. These data suggest that the biliary clearance of pitavastatin can be largely accounted for by BCRP in mice. In the case of humans, transcellular transport of pitavastatin was determined in the Madin-Darby canine kidney II cells expressing OATP1B1 and human canalicular efflux transporters. A significant basal-to-apical transport of pitavastatin was observed in OATP1B1/MDR1 and OATP1B1/MRP2 double transfectants as well as OATP1B1/BCRP double transfectants, implying the involvement of multiple transporters in the biliary excretion of pitavastatin in humans. This is in contrast to a previous belief that the biliary excretion of statins is mediated mainly by MRP2.

The liver plays an important role in the excretion of xenobiotics, including many kinds of drugs. A number of reports have shown that several kinds of transporters are expressed on the canalicular membrane in the liver for the efficient elimination of drugs via the bile (Chandra and Brouwer, 2004). It has been generally accepted that transport of various organic anions across the canalicular membrane is mainly mediated by multidrug resistance-associated protein 2 (MRP2/ABCC2), whereas the bile salt export pump (BSEP/ABCB11) exclusively accepts bile acids, and multidrug resistance protein (P-glycoprotein, MDR1/ABCB1) can transport relatively hydrophobic neutral or cationic compounds (Chandra and Brouwer, 2004). However, several reports have shown that some anionic drugs can also be recognized by BSEP and MDR1 (Cvetkovic et al., 1999; Hirano et al., 2005), suggesting that multiple transport mechanisms are involved in the biliary excretion of organic anions.

Moreover, breast cancer resistance protein (BCRP/ABCG2) has been cloned recently and can accept various kinds of organic anions, especially sulfated conjugates of steroids and xenobiotics (Allikmets et al., 1998; Suzuki et al., 2003). Because BCRP is expressed on the bile canalicular membrane of hepatocytes as well as the brush-border membrane of enterocytes, trophoblast cells in placenta, and the apical membrane of lactiferous ducts in the mammary gland (Maliepaard et al., 2001), BCRP must also be considered as one of the routes for the biliary excretion of organic anions. Current evidence indicates that BCRP contributes to the membrane transport of some substrates, such as intestinal absorption and transfer to breast milk (Jonker et al., 2000, 2002; Adachi et al., 2004; Mizuno et al., 2004; Kondo et al., 2005; Merino et al.,

This work was supported by a Health and Labor Sciences Research Grants from Ministry of Health, Labor, and Welfare for the Research on Advanced Medical Technology.

Article, publication date, and citation information can be found at http://molpharm.aspetjournals.org.

doi:10.1124/mol.105.014019.

ABBREVIATIONS: MRP (Mrp), multidrug resistance-associated protein; OATP (Oatp), organic anion transporting polypeptide; BCRP (Bcrp), breast cancer resistance protein; BSEP (Bsep), bile salt export pump; MDR (Mdr), multidrug resistance protein; HEK, human embryonic kidney; MDCK, Madin-Darby canine kidney; HMG-CoA, 3-hydroxy-3-methylglutaryl-coenzyme A; $E_2$17βG, 17β-estradiol-17β-D-glucuronide; EHBR, Eisai hyperbilirubinemic rat; LC/MS, high-performance liquid chromatography/mass spectrometry; GFP, green fluorescent protein; SNP, single nucleotide polymorphism; TS, Tris-HCl and sucrose; PE, polyethylene.

2005a). Regarding the involvement of BCRP in biliary excretion, some reports have demonstrated that the biliary excretion of 2-amino-1-methyl-6-phenylimidazo(4,5-*b*)pyridine and nitrofurantoin is almost impaired in Bcrp1(−/−) mice (van Herwaarden et al., 2003; Merino et al., 2005a) and that the biliary excretion of topotecan and cimetidine is also mainly regulated by Bcrp, considering the gender difference in the hepatic expression level of Bcrp and the plasma concentration profiles (Merino et al., 2005b). In addition, it has been demonstrated that certain kinds of single-nucleotide polymorphisms (SNPs) in BCRP and inhibition of BCRP-mediated transport by some compounds may alter its function and the pharmacokinetics of some drugs in vitro (Imai et al., 2002; Zamber et al., 2003; Kondo et al., 2004) as well as in vivo (Kruijtzer et al., 2002; Sparreboom et al., 2004). Therefore, the pharmacokinetics of several important compounds are regulated mainly by BCRP.

Pitavastatin is a highly potent inhibitor of 3-hydroxymethylglutaryl coenzyme A (HMG-CoA) reductase, the rate-limiting enzyme in cholesterol biosynthesis (Kajinami et al., 2003). Pitavastatin causes a significant reduction in not only serum total cholesterol and low-density lipoprotein cholesterol but also triglyceride levels (Stein et al., 1998). It has been demonstrated that [^{14}C]pitavastatin is distributed selectively to the liver in rats with a liver-to-plasma concentration ratio of more than 50 (Kimata et al., 1998). We demonstrated previously that pitavastatin is taken up into human hepatocytes mainly by OATP1B1 (OATP2/OATP-C) (Hirano et al., 2004). Then, because it is scarcely metabolized in human liver microsomes (Fujino et al., 2003), pitavastatin is supposed to be excreted into bile in unchanged form (Kojima et al., 2001). However, the biliary transport mechanism of pitavastatin has not been clarified yet. So far, Fujino et al. (2002) have demonstrated that after intravenous bolus administration of pitavastatin, its plasma concentration and biliary excretion in Eisai hyperbilirubinemic rats (EHBRs), an Mrp2-deficient rat, are comparable with those in Sprague-Dawley rats and that the plasma and brain concentrations of pitavastatin in mdr1a/1b knockout mice are not different from those in control mice. In addition, we have already shown that pitavastatin is not a substrate of rat and human BSEP (Hirano et al., 2005). These results suggest that BSEP, MRP2, and MDR1 do not make a major contribution to the biliary excretion of pitavastatin.

In the present study, to demonstrate the involvement of BCRP in the biliary excretion of pitavastatin, we examined the transport of pitavastatin by transporter expression systems and observed the biliary excretion clearance of pitavastatin in transporter-deficient animals. Moreover, to check whether other statins could be substrates of BCRP or not, we performed a transport study using BCRP-expressing membrane vesicles.

Materials and Methods

Animals. Male Bcrp1(−/−) and wild-type FVB mice (16–18 weeks old) were used in the present study (Jonker et al., 2002). Male Sprague-Dawley rats (7–8 weeks old) and EHBRs (7–8 weeks old) were purchased from Nippon SLC (Shizuoka, Japan). All animals were maintained under standard conditions with a reverse dark-light cycle and were treated humanely. Food and water were available ad libitum. The studies reported in this manuscript were carried out in accordance with the guidelines provided by the Institutional Animal Care Committee (Graduate School of Pharmaceutical Sciences, The University of Tokyo, Tokyo, Japan).

Materials. Pitavastatin, monocalcium bis[(3*R*,5*S*,6*E*)-7-[2-cyclopropyl-4-(4-fluorophenyl)-3-quinolyl]3,5-dihydroxy-6-hepteonate] was synthesized by Nissan Chemical Industries (Chiba, Japan). [^{3}H]Pitavastatin (16.0 Ci/mmol) and [^{3}H]cerivastatin (4.86 Ci/mmol) were synthesized by Amersham Biosciences UK, Ltd. (Little Chalfont, Buckinghamshire, UK) and Hartmann Analytic GmbH (Braunschweig, Germany), respectively. [^{3}H]Pravastatin (44.6 Ci/mmol), [^{14}C]fluvastatin (45.7 mCi/mmol), and [^{3}H]rosuvastatin (79 Ci/mmol) were supplied by Sankyo Co., Ltd. (Tokyo, Japan), Novartis Pharma K.K. (Basel, Switzerland), and AstraZeneca PLC (London, UK), respectively. Other unlabeled HMG-CoA reductase inhibitors (atorvastatin, cerivastatin, fluvastatin, pravastatin, rosuvastatin, and simvastatin acid) were donated by Kowa Co., Ltd. (Tokyo, Japan). [^{3}H]17β-Estradiol-17β-D-glucuronide ($E_2$17βG) and [^{3}H]estrone-3-sulfate (45 and 46 Ci/mmol, respectively) were purchased from PerkinElmer Life and Analytical Sciences (Boston, MA). Unlabeled $E_2$17βG and estrone-3-sulfate were purchased from Sigma-Aldrich (St. Louis, MO). All other chemicals were of analytical grade and were commercially available.

Cell Culture. Human BCRP-, mouse Bcrp-, or green fluorescent protein (GFP)-transfected HEK293 cells (Kondo et al., 2004) and MDCK II single- and double-transfected cells expressing human OATP1B1, MDR1, MRP2, or BCRP (Matsushima et al., 2005) and rat Oatp1b2 or Mrp2 (Sasaki et al., 2004) were grown in Dulbecco's modified Eagle's medium low glucose (Invitrogen, Carlsbad, CA) supplemented with 10% fetal bovine serum (Sigma-Aldrich), 100 U/ml penicillin, and 100 μg/ml streptomycin at 37°C with 5% CO_2 and at 95% humidity.

Construction and Infection of Recombinant Adenovirus and the Membrane-Vesicle Preparation. Details of the procedure for producing recombinant adenovirus containing human BCRP, mouse Bcrp, and GFP have been described previously (Kondo et al., 2004). Membrane vesicles were prepared from BCRP and GFP-transfected HEK293 cells according to the method described previously (Kondo et al., 2004). For the preparation of the isolated membrane vesicles, HEK293 cells cultured in a 15-cm dish were infected by recombinant adenovirus containing human and mouse BCRP cDNA (multiplicity of infection = 10). As a negative control, cells were infected with GFP (multiplicity of infection = 10). Cells were harvested 48 h after infection, and then the membrane vesicles were isolated from 1 to 2 × 10^8 cells using a standard method described previously in detail (Muller et al., 1994). In brief, cells were diluted 40-fold with hypotonic buffer (1 mM Tris-HCl and 0.1 mM EDTA, pH 7.4, at 37°C) and stirred gently for 1 h on ice in the presence of 2 mM phenylmethylsulfonyl fluoride, 5 μg/ml leupeptin, 1 μg/ml pepstatin, and 5 μg/ml aprotinin. The cell lysate was centrifuged at 100,000*g* for 30 min at 4°C, and the resulting pellet was suspended in 10 ml of isotonic TS buffer (10 mM Tris-HCl and 250 mM sucrose, pH 7.4 at 4°C) and homogenized using a Dounce B homogenizer (glass/glass, tight pestle, 30 strokes). The crude membrane fraction was layered on top of 38% (w/v) sucrose solution in 5 mM Tris-HEPES, pH 7.4, at 4°C, and centrifuged in Beckman SW41 rotor centrifuged at 280,000*g* for 60 min at 4°C. The turbid layer at the interface was collected, diluted to 23 ml with TS buffer, and centrifuged at 100,000*g* for 30 min at 4°C. The resulting pellet was suspended in 400 μl of TS buffer. Vesicles were formed by passing the suspension 30 times through a 27-gauge needle using a syringe. The membrane vesicles were finally frozen in liquid nitrogen and stored at −80°C until use. Protein concentrations were determined by the Lowry method, and bovine serum albumin was used as a standard.

Transport Studies with Membrane Vesicles. The transport studies were performed using a rapid filtration technique (Hirohashi et al., 1999). In brief, 15 μl of transport medium (10 mM Tris-HCl, 250 mM sucrose, and 10 mM $MgCl_2$, pH 7.4) containing radiolabeled compounds, with or without unlabeled substrate, was preincubated

at 37°C for 3 min and then rapidly mixed with 5 μl of membrane vesicle suspension (5 μg of protein). The reaction mixture contained 5 mM ATP or AMP along with the ATP-regenerating system (10 mM creatine phosphate and 100 μg/μl creatine phosphokinase). The transport reaction was terminated by the addition of 1 ml of ice-cold buffer containing 10 mM Tris-HCl, 250 mM sucrose, and 0.1 M NaCl, pH 7.4. The stopped reaction mixture was filtered through a 0.45-μm hemagglutinin filter (Millipore Corporation, Billerica, MA) and then washed twice with 5 ml of stop solution. Radioactivity retained on the filter was determined in a liquid scintillation counter (LS6000SE; Beckman Coulter, Inc., Fullerton, CA) after the addition of scintillation cocktail (Clear-sol I; Nacalai Tesque, Tokyo, Japan).

Transcellular Transport Study. Transfected MDCK II cells were seeded in 24-well plates at a density of 1.4×10^5 cells/well and were cultured with 10 mM sodium butyrate for 24 h before the transport study (Sasaki et al., 2002). Krebs-Henseleit buffer consisted of 142 mM NaCl, 23.8 mM Na_2CO_3, 4.83 mM KCl, 0.96 mM KH_2PO_4, 1.20 mM $MgSO_4$, 12.5 mM HEPES, 5 mM glucose, and 1.53 mM $CaCl_2$ adjusted to pH 7.4. The experiments were initiated by replacing the medium on either the apical or basal side of the cell layer with complete medium containing tritium-labeled and unlabeled $E_2$17βG or pitavastatin (0.1 μM). The cells were incubated at 37°C, and aliquots of medium were taken from each compartment at designated time points. Radioactivity in 100 μl of medium was measured in a liquid scintillation counter (LS6000SE; Beckman Coulter) after the addition of scintillation cocktail (Clear-sol I; Nacalai Tesque). At the end of the experiments, the cells were washed three times with 1.5 ml of ice-cold Krebs-Henseleit buffer and solubilized in 450 μl of 0.2 N NaOH. After the addition of 225 μl of 0.4 N HCl, 600-μl aliquots were transferred to scintillation vials. Aliquots (50 μl) of cell lysate were used to determine protein concentrations as described above.

Kinetic Analysis. Ligand uptake was normalized in terms of the amount of membrane protein and expressed as the uptake volume [μl/mg protein], given as the amount of radioactivity associated with the cells [dpm/mg protein] divided by its concentration in the incubation medium [dpm/μl]. The ATP-dependent uptake of ligands via BCRP was calculated by subtracting the ligand in the presence of AMP from that in the presence of ATP. Kinetic parameters were obtained using the equation $v = (V_{max} \times S)/(K_m + S)$, where v is the uptake velocity of the substrate (in picomoles per minute per milligram of protein), S is the substrate concentration in the medium (in micromolars), K_m is the Michaelis constant (in micromolars), and V_{max} is the maximum uptake velocity (in picomoles per minute per milligram of protein). The Damping Gauss Newton Method algorithm was used with a MULTI program (Yamaoka et al., 1981) to perform nonlinear least-squares data fitting. Inhibition constants (K_i) of a series of compounds were calculated with the use of the following equation (if the substrate concentration was much lower than the K_m value): $CL(+I) = CL/(1 + I/K_i)$, where CL represents the uptake clearance in the absence of inhibitor, $CL(+I)$ represents the uptake clearance in the presence of inhibitor, and I represents the concentration of the inhibitor. When fitting the data to determine the K_i value, the input data were weighed as the reciprocal of the observed values.

In Vivo Infusion Study in Rats. Male Sprague-Dawley rats and EHBRs weighing approximately 250 to 300 g were used for these experiments. Under pentobarbital anesthesia (30 mg/kg), the femoral vein was cannulated with a polyethylene catheter (PE-50) for the injection of [^{3}H]pitavastatin. The bile duct was cannulated with a polyethylene catheter (PE-10) for bile collection. The rats received a constant infusion of pitavastatin at a dose of 72 μg/h/kg after a bolus intravenous administration of 0.25 mg/kg. Blood samples were collected from the jugular vein. Bile was collected in preweighed test tubes at 30-min intervals throughout the experiment. Plasma was prepared by centrifugation of the blood samples (10,000*g*, Microfuge; Beckman Coulter). The rats were killed after 210 min, and the entire liver was excised immediately. Then the liver was weighed and minced, and subsequently 200 μl of hydroxyperoxide and 400 μl of isopropanol were added to approximately 200 mg of liver. This was incubated at 55°C for 4 to 6 h after the addition of 2 ml of soluene (PerkinElmer Life and Analytical Sciences) to dissolve the tissues, and then the radioactivity was determined in a liquid scintillation counter after the addition of scintillation cocktail.

In Vivo Infusion Study in Mice and Quantification of Pitavastatin by LC/MS. Male FVB and Bcrp1(−/−) mice weighing approximately 28 to 33 g were used throughout these experiments. Under pentobarbital anesthesia (30 mg/kg), the jugular vein was cannulated with a polyethylene catheter (PE-10) for the injection of pitavastatin. The bile duct was cannulated with a polyethylene catheter (SP-8) for bile collection. The mice received a constant infusion of pitavastatin at a dose of 300 μg/h/kg. Blood samples were collected from the opposite jugular vein. Bile was collected in preweighed test tubes at 15-min intervals throughout the experiments. Plasma was prepared by centrifugation of the blood samples. The mice were killed after 150 min, and the entire liver, kidney, brain, and skeletal muscle were excised immediately. The tissues were weighed and stored at −80°C until quantification. Portions of liver, kidney, brain, and skeletal muscle were added to five volumes of physiological saline (w/v) and homogenized. Plasma (10 μl), bile (1 μl), or tissue homogenate (10 or 100 μl) was deproteinized with 200 μl of methanol containing the internal standard (40 ng/ml atorvastatin), followed by centrifugation at 4°C and 10,000*g* for 10 min. The supernatant (100 μl) was mixed with 50 μl of water and subjected to high-performance liquid chromatography (Waters 2695; Waters, Milford, MA). The LC/MS analysis of pitavastatin was performed using an Inertsil ODS-3 column (50 × 2.1 mm; particle size, 5 μm) (GL Sciences, Tokyo, Japan). The mobile phase consisted of methanol/ammonium formate buffer, pH 4 = 7:3 (v/v), and the flow rate was 0.7 ml/min. The MS instrument used for this work was a ZQ micromass (Waters) equipped with a Z-spray source; it was operated in the positive-ion electrospray ionization mode. The Z-spray desolvation temperature, capillary voltage, and cone voltage were 350°C, 3400 V, and 40 V, respectively. The *m/z* monitored for pitavastatin and atorvastatin was 422.3 and 559.0, respectively. No chromatographic interference was found for pitavastatin and atorvastatin in extracts from blank plasma, bile, and tissue homogenates. The retention times of pitavastatin and atorvastatin were 1.2 and 1.1 min, respectively. The detection limits for pitavastatin were 5, 2000, 100, 5, 5, and 5 ng/ml in plasma, bile, liver, kidney, brain, and muscle, respectively.

Pharmacokinetic Analysis. Total plasma clearance (CL_{total}), biliary clearance normalized by circulating plasma ($CL_{bile,plasma}$), and biliary clearance normalized by the liver concentration ($CL_{bile,liver}$) were calculated from the equations $CL_{total} = I/C_{ss,plasma}$, $CL_{bile,plasma} = V_{bile}/C_{ss,plasma}$, and $CL_{bile,\ liver} = V_{bile}/C_{ss,liver}$, where I, $C_{ss,plasma}$, V_{bile}, and $C_{ss,liver}$ represent the infusion rate (in micrograms per minute per kilogram), plasma concentrations at steady state (in nanograms per milliliter), biliary excretion rate at steady state (in micrograms per minute per kilogram), and hepatic concentration at steady state (in nanograms per milliliter), respectively. In rats, $C_{ss,plasma}$ was determined as the mean value of the plasma [^{3}H]pitavastatin concentrations at 60, 90, 120, 150, 180, and 210 min. V_{bile} was determined as the mean value of the biliary excretion rate of [^{3}H]pitavastatin from 60 to 90 min, from 90 to 120 min, from 120 to 150 min, from 150 to 180 min, and from 180 to 210 min. In mice, $C_{ss,plasma}$ was determined as the mean value of the plasma unlabeled pitavastatin concentrations at 90, 120, and 150 min. V_{bile} was determined as the mean value of the biliary excretion rate of unlabeled pitavastatin from 90 to 105 min, from 105 to 120 min, from 120 to 135 min, and from 135 to 150 min. $C_{ss,liver}$ was determined as the hepatic pitavastatin concentration at the end of the in vivo experiment. To calculate $C_{ss,liver}$, the specific gravity of the liver was assumed to be unity. Thus, the amount in the liver (nanograms per gram of liver) can be regarded as the hepatic concentration (nanograms per gram), and the units of $CL_{bile,liver}$ are in milliliters per minute per kilogram.

Statistical Analysis. Statistically significant differences were determined using one-way analysis of variance followed by Fisher's least significant difference method. Differences were considered to be significant at $P < 0.05$.

Results

ATP-Dependent Uptake of [^{3}H]Pitavastatin into BCRP-Expressing Membrane Vesicles. The time profiles and Eadie-Hofstee plots for the uptake of [^{3}H]pitavastatin by BCRP-expressing membrane vesicles are shown in Fig. 1. The uptake of [^{3}H]pitavastatin into membrane vesicles from human and mouse BCRP-transfected HEK293 cells was markedly stimulated by ATP but not that into GFP-transfected control cells (Fig. 1, A and B). The concentration-dependence of human and mouse BCRP-mediated ATP-dependent uptake of pitavastatin is shown in Fig. 1, C and D. The K_m and V_{max} values for the ATP-dependent uptake of pitavastatin were 5.73 ± 1.52 μM and 1106 ± 79 pmol/min/mg protein by human BCRP and 4.77 ± 0.50 μM and 881 ± 20 pmol/min/mg protein by mouse Bcrp, respectively.

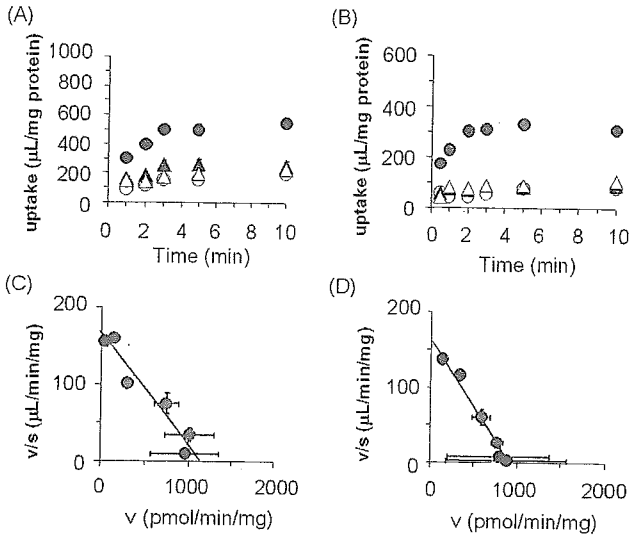

Fig. 1. Time profiles and Eadie-Hofstee plots of the uptake of [^{3}H]pitavastatin by human and mouse BCRP-expressing membrane vesicles. The uptake of 0.1 μM [^{3}H]pitavastatin by human BCRP (hBCRP) (A) and mouse Bcrp (mBcrp) (B), respectively, was examined at 37°C in medium containing 5 mM ATP (closed symbols) or AMP (open symbols). Circles and triangles represent the uptake in hBCRP- (or mBcrp-) and GFP-expressing membrane vesicles, respectively. The hBCRP- (C) and mBcrp (D)-mediated uptake of [^{3}H]pitavastatin was determined for 2 and 1 min, respectively. Each point represents the mean ± S.E. (n = 3). Where vertical bars are not shown, the S.E. values are within the limits of the symbols. The data were fitted to the Michaelis-Menten equation by nonlinear regression analysis, as described under *Materials and Methods*, and each solid line represents the fitted curve.

Uptake of Other Statins into BCRP-Expressing Membrane Vesicles. Uptake of other statins into human and mouse BCRP-expressing membrane vesicles was observed (Fig. 2). We did not see any significant ATP-dependent uptake of cerivastatin and fluvastatin by mouse Bcrp-expressing membrane vesicles compared with GFP-transfected vesicles, whereas human BCRP significantly recognized all of the statins we tested (cerivastatin, fluvastatin, pitavastatin, pravastatin, and rosuvastatin) as a substrate (Fig. 2, A–E). Estrone-3-sulfate (0.1 μM), which was a positive control compound for BCRP-mediated transport, was accepted as a substrate of both human and mouse BCRP (Fig. 2F). The K_m value of estrone-3-sulfate by mouse Bcrp was 16.4 ± 3.0 μM (data not shown).

Inhibitory Effects of Statins on the ATP-Dependent Uptake of [^{3}H]Estrone-3-sulfate into Human and Mouse BCRP-Expressing Membrane Vesicles. The inhibitory effects of statins on the ATP-dependent uptake of [^{3}H]estrone-3-sulfate by human and mouse BCRP-expressing membrane vesicles were observed. All of the statins except for pravastatin (~300 μM), inhibited the ATP-dependent uptake of [^{3}H]estrone-3-sulfate by human and mouse BCRP in a dose-dependent manner. The K_i values of statins for human and mouse BCRP are summarized in Table 1.

Transcellular Transport of Pitavastatin across Double Transfectants. Transcellular transport of pitavastatin across double-transfected MDCK II monolayers expressing uptake transporter (OATP1B1) and efflux transporter (MDR1, MRP2, or BCRP) was compared with that across the single-transfected monolayer and the vector-transfected con-

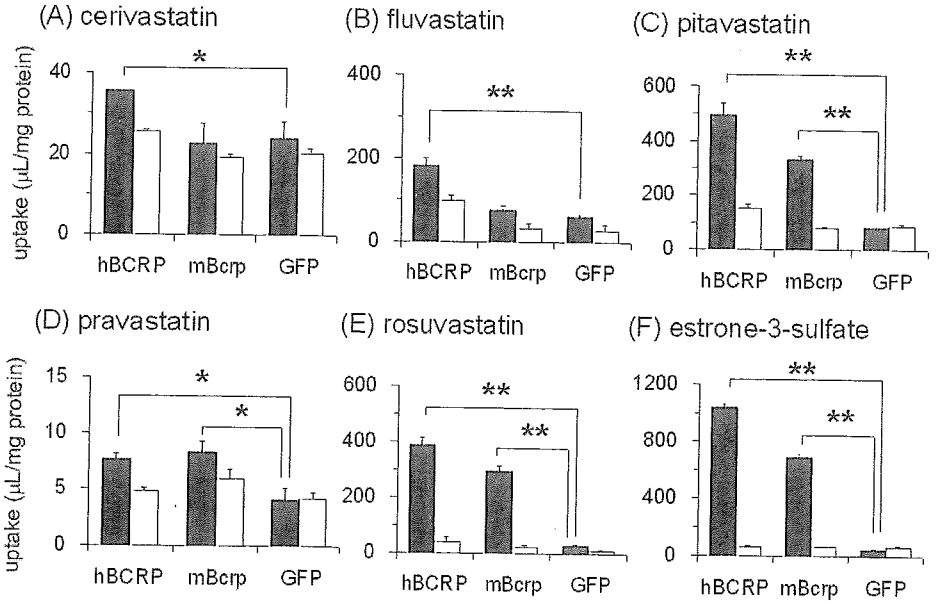

Fig. 2. The ATP-dependent uptake of statins by human BCRP (hBCRP)-, mouse Bcrp (mBcrp)-, and GFP-expressing membrane vesicles. The uptake of 0.1 μM [^{3}H]cerivastatin (A), 5 μM [^{14}C]fluvastatin (B), 0.1 μM [^{3}H]pitavastatin (C), 0.1 μM [^{3}H]pravastatin (D), and 0.1 μM [^{3}H]rosuvastatin (E) for 5 min and 0.1 μM [^{3}H]estrone-3-sulfate (F) for 2 min, respectively, was determined at 37°C in medium in the presence of 5 mM ATP (■) or AMP (□). Each point represents the mean ± S.E. (n = 3). *, $P < 0.05$; **, $P < 0.01$

trol monolayer. In the case of humans, as shown in Fig. 3, a symmetrical flux of pitavastatin was observed across the control, MDR1-, MRP2-, and BCRP-expressing MDCK II monolayer. The basal-to-apical flux of pitavastatin across the OATP1B1-expressing monolayer was approximately twice that in the opposite direction, whereas the basal-to-apical flux of pitavastatin was approximately 15, 110, and 230 times higher than that in the opposite direction in OATP1B1/MRP2, OATP1B1/BCRP, and OATP1B1/MDR1 double-transfected cells, respectively. In addition, transcellular transport of pitavastatin across double-transfected MDCK II monolayers expressing rat Oatp1b2 and Mrp2 was also compared with that across the Oatp1b2 or Mrp2 single-transfected monolayer and the vector-transfected control monolayer. The basal-to-apical flux of pitavastatin was 2.4 times higher than that in the opposite direction in the Oatp1b2/Mrp2 double-transfected cells, although a smaller vectorial transport was observed even in the Oatp1b2-expressing monolayer (Fig. 4). In both rats and humans, we checked the transcellular transport of $E_2 17\beta G$ as a positive control in parallel and obtained results similar to those measured previously (Matsushima et al., 2005; data not shown).

TABLE 1

Inhibitory effects of statins on the ATP-dependent uptake of [^{3}H]estrone-3-sulfate by human BCRP- and mouse Bcrp-expressing membrane vesicles

The ATP-dependent uptake of [^{3}H]estrone-3-sulfate (0.1 μM) for 1 min by human BCRP (hBCRP) and mouse Bcrp (mBcrp) was determined in the presence and absence of unlabeled statins at the designated concentrations. The values are expressed as a percentage of the ATP-dependent uptake of [^{3}H]estrone-3-sulfate in the absence of any unlabeled compounds. The ATP-dependent uptake was obtained by subtracting the transport velocity in the presence of AMP from that in the presence of ATP. The K_i values were determined by fitting the data using the non-least squares method. The values are expressed as mean ± computer-calculated S.D. (n = 3).

Statins	hBCRP	mBcrp
	μM	
Atorvastatin	14.3 ± 1.9	17.6 ± 1.7
Cerivastatin	18.1 ± 2.5	30.1 ± 6.3
Fluvastatin	5.43 ± 0.27	8.62 ± 0.86
Pitavastatin	2.92 ± 0.35	6.00 ± 0.71
Pravastatin	>300 μM	>300 μM
Rosuvastatin	15.4 ± 2.4	10.3 ± 0.6
Simvastatin acid	18.0 ± 4.3	24.9 ± 3.8

Plasma, Liver Concentration and Biliary Excretion Profiles at Steady State in Sprague-Dawley Rats and EHBRs. It has been reported that pitavastatin is not significantly metabolized in rats, and 70% of the excreted amount in bile can be detected in unchanged form (Fujino et al., 2002). Therefore, we used [^{3}H]pitavastatin in rats in an in vivo study to examine the involvement of Mrp2 in the biliary excretion of pitavastatin. The plasma concentration of pitavastatin reached a plateau at 60 min during constant infusion after a bolus intravenous administration. The biliary excretion rate (V_{bile}), the steady-state plasma concentration ($C_{ss,plasma}$), and total clearance (CL_{total}) values of pitavastatin in EHBRs were almost the same as those in normal rats (Fig. 5 and Table 2). The concentration of pitavastatin and the K_p value in the liver at steady state in EHBRs were lower than those in normal rats, and the $CL_{bile,plasma}$ and $CL_{bile,\ liver}$ values in EHBRs were slightly higher than those in normal rats, although the differences were not statistically significant (Fig. 5).

Plasma, Tissue Concentration, and Biliary Excretion Profiles at Steady State in FVB and Bcrp1(−/−) Mice. The plasma concentration of pitavastatin reached a plateau at 90 min during constant infusion (Fig. 6). The V_{bile} of parent pitavastatin in Bcrp1(−/−) mice was much lower than that in control mice, whereas the $C_{ss,plasma}$ and CL_{total} values of pitavastatin in Bcrp1(−/−) mice did not differ from those in normal mice (Table 3). The K_p values of pitavastatin in the kidney, brain, and skeletal muscle as well as the liver (Table 3) at steady state were similar in control and Bcrp1(−/−) mice (K_p value for kidney, 1.41 ± 0.10 and 1.48 ±0.12 ng/g; for brain, 0.0308 ± 0.0027 and 0.0322 ± 0.0070 ng/g; and for skeletal muscle, 0.0985 ± 0.0075 and 0.0960 ± 0.0061 ng/g in wild-type and Bcrp1(−/−) mice, respectively).

Discussion

Pitavastatin, a new potent inhibitor of HMG-CoA reductase, is scarcely metabolized in humans and is believed to be excreted into the bile in intact form. In the present study, we concentrated on a new candidate transporter, BCRP, for the biliary excretion of pitavastatin.

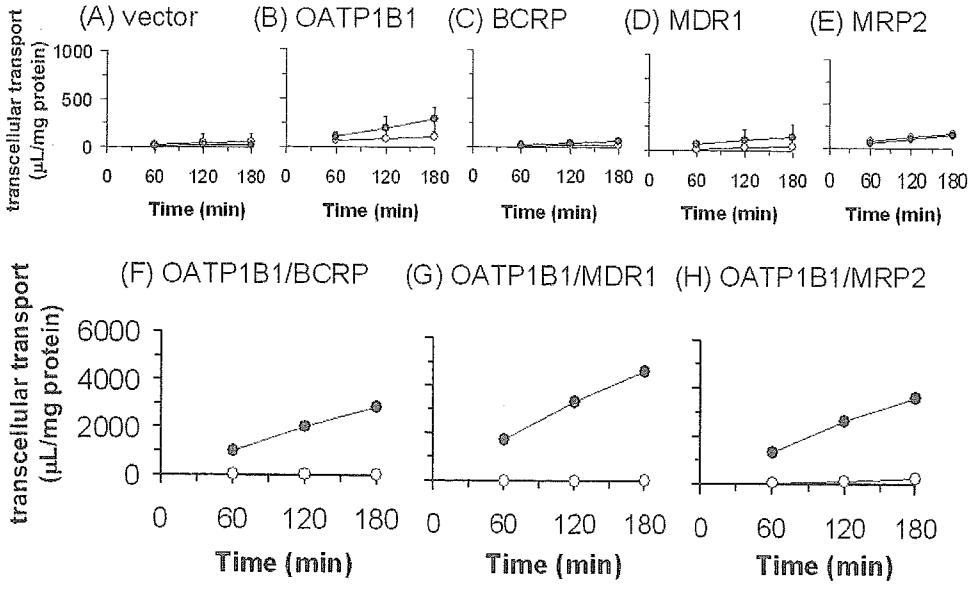

Fig. 3. Time profiles for the transcellular transport of [^{3}H]pitavastatin across MDCK II monolayers expressing human transporters. Transcellular transport of [^{3}H]pitavastatin (0.1 μM) across MDCK II monolayers expressing OATP1B1 (B), BCRP (C), MDR1 (D), MRP2 (E), both OATP1B1 and BCRP (F), both OATP1B1 and MDR1 (G), and both OATP1B1 and MRP2 (H) was compared with that across the vector-transfected control MDCK II monolayer (A). ○ and ● represent the transcellular transport in the apical-to-basal and basal-to-apical direction, respectively. Each point represents the mean ± S.E. (n = 3). Where vertical bars are not shown, the S.E. values are within the limits of the symbols.

ATP-dependent uptake of pitavastatin in human and mouse BCRP-expressing membrane vesicles was observed (Fig. 1). The K_m value of pitavastatin for human BCRP (5.73 μM) was almost the same as that for mouse Bcrp (4.77 μM), and these K_m values were similar to that of estrone-3-sulfate, which is a well-known substrate of human BCRP (Suzuki et al., 2003), indicating that pitavastatin is also a good substrate of BCRP. Regarding other statins, as shown in Table 1, no species difference in the K_i value of each statin for the BCRP-mediated uptake of estrone-3-sulfate was observed between humans and mice. The inhibition potency of statins, except for pravastatin, was almost identical, whereas pravastatin could not inhibit the BCRP-mediated transport of estrone-3-sulfate up to 300 μM. On the other hand, all statins we tested could be substrates of human BCRP, whereas four of them were also substrates of mouse Bcrp (Fig. 2). From a pharmacokinetic viewpoint, BCRP could at least partly contribute to the biliary excretion of pravastatin, pitavastatin, and rosuvastatin, which are scarcely metabolized by metabolic enzymes like cytochrome P450 in the liver. On the other hand, in the case of atorvastatin, cerivastatin, and simvastatin, which have been reported to be extensively metabolized by cytochrome P450 enzymes (Garcia et al., 2003), the biliary excretion of their unchanged form via BCRP was considered to be minor in in vivo situations.

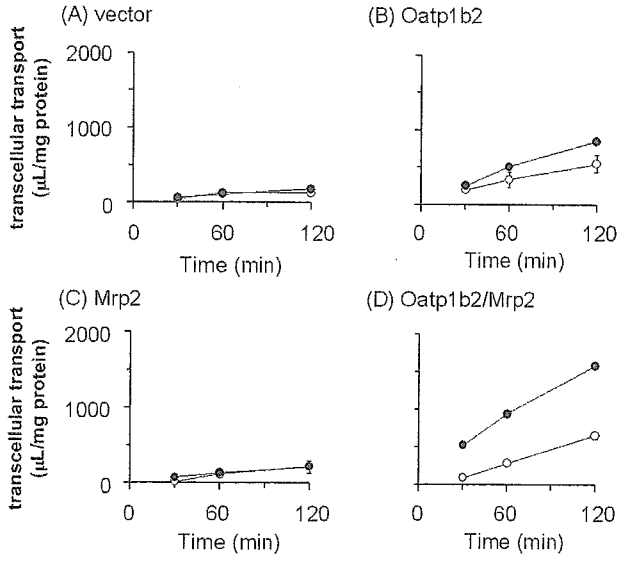

Fig. 4. Time profiles for the transcellular transport of [^{3}H]pitavastatin across MDCK II monolayers expressing rat transporters. Transcellular transport of [^{3}H]pitavastatin (0.1 μM) across MDCK II monolayers expressing Oatp1b2 (B), Mrp2 (C), and both Oatp1b2 and Mrp2 (D) was compared with that across the vector-transfected control MDCK II monolayer (A). ○ and ● represent the transcellular transport in the apical-to-basal and basal-to-apical direction, respectively. Each point represents the mean ± S.E. (n = 3). Where vertical bars are not shown, the S.E. values are within the limits of the symbols.

To estimate the contribution of each transporter to the biliary excretion of pitavastatin in the in vivo study, the biliary excretion of pitavastatin at steady state was investigated using Mrp2- and Bcrp1-deficient animals. Because pitavastatin was found to be scarcely metabolized in rats (Fujino et al., 2002), the radioactivity would reflect the parent pitavastatin. We confirmed that the plasma concentration and biliary excretion rate of pitavastatin was not changed between Sprague-Dawley rats and EHBRs (Fig. 5 and Table. 2), which is consistent with a previous report (Fujino et al., 2002). Therefore, the involvement of Mrp2 in the biliary excretion of pitavastatin is minor. The liver concentration in EHBRs was significantly lower than that in control rats possibly because of the accelerated efflux via the basolateral membrane in the liver caused by the induction of Mrp3 (Ogawa et al., 2000) and the inhibition of hepatic uptake process from the blood by a higher concentration of bilirubin glucuronide in EHBRs (Sathirakul et al., 1993), or by the decrease in the expression levels of transporters responsible for the uptake of pitavastatin.

Biliary excretion of pitavastatin was also observed in Bcrp1(−/−) and control mice. In contrast to humans and rats, pitavastatin is extensively metabolized in mice, so we decided to quantify the unchanged form separately by LC/MS in mice. The biliary excretion clearance of pitavastatin in Bcrp1(−/−) mice was 10 times lower than that in control mice, suggesting that unchanged pitavastatin is excreted into bile mainly by Bcrp. In control mice, the biliary clear-

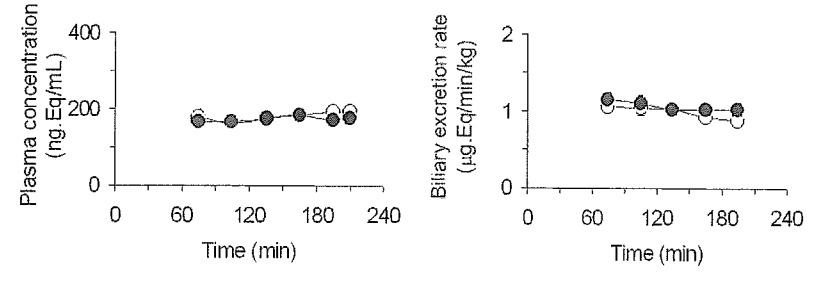

Fig. 5. Plasma concentrations and biliary excretion rate of [^{3}H]pitavastatin during constant intravenous infusion into Sprague-Dawley rats and EHBRs. The plasma concentration (A) and biliary excretion rate (B) of total radioactivity were determined during constant intravenous infusion into Sprague-Dawley rats (○) and EHBRs (●). Each point plotted, with its vertical bar, represents the mean ± S.E. of four rats.

TABLE 2

Pharmacokinetic parameters of pitavastatin during constant intravenous infusion into Sprague-Dawley (SD) rats and EHBRs

Data represent the mean ± S.E. (n = 4).

	$C_{ss,plasma}$	CL_{total}	$CL_{bile,plasma}$	$CL_{bile,liver}$	Liver Concentration	$K_{p,liver}$
	ng · Eq/ml	*ml/min/kg*	*ml/min/kg*	*ml/min/kg*	*ng · Eq/g*	
SD rat	195 ± 13	6.26 ± 0.49	4.55 ± 0.13	0.248 ± 0.042	4346 ± 406	23.0 ± 3.6
EHBR	179 ± 8	6.75 ± 0.34	5.77 ± 0.53	0.399 ± 0.049	2621 ± 139**	14.7 ± 0.8

** $P < 0.01$.

$C_{ss,plasma}$, plasma steady-state concentration (mean of plasma concentration at 210 min); CL_{total}, total plasma clearance obtained by dividing the infusion rate by $C_{ss,plasma}$; $CL_{bile,plasma}$, biliary clearance normalized by the plasma concentration; $CL_{bile,liver}$, biliary clearance normalized by the liver concentration; $K_{p,liver}$, K_p value obtained by dividing the liver concentration by $C_{ss,plasma}$ (at 210 min).

ance normalized by plasma concentration ($CL_{bile,plasma}$) accounted for only 5% of the plasma total clearance (CL_{total}), indicating that pitavastatin is mainly excreted into bile as metabolites. Taking extensive metabolism into consideration, it is natural that the plasma and liver concentrations were not different between Bcrp1(−/−) and control mice, even if the biliary clearance of the parent compound was drastically reduced in Bcrp1(−/−) mice. In contrast to mice, pitavastatin is believed to be excreted into the bile in an intact form with only minimal metabolism in humans (Fujino et al., 2003). Therefore, BCRP is estimated to be involved in the biliary excretion of pitavastatin in humans. On the other hand, a previous in vivo study using EHBRs revealed that Mrp2 is a major transporter for the excretion of pravastatin in rats (Yamazaki et al., 1997). Even though pitavastatin and pravastatin belong to the same category, HMG-CoA reductase inhibitors, it was interesting to find that pitavastatin and pravastatin are excreted into the bile by different efflux transport systems. In the brain and kidney, in which BCRP is also expressed, and skeletal muscle, which is a target site of severe adverse effects of statins (rhabdomyolysis), these tissue concentrations were not significantly different between Bcrp1(−/−) and control mice. Thus, Bcrp does not contribute to the distribution of pitavastatin in these tissues. BCRP was expressed not only in the liver, kidney, and brain, but also in the small intestine and mammary gland (Doyle and Ross, 2003). It has been demonstrated that BCRP critically modulates the absorption of certain drugs from the small intestine and transfer to milk (Adachi et al., 2004; Merino et al., 2005a). Further studies are needed to clarify the importance of BCRP in the intestinal absorption and tissue distribution of a series of statins.

In Fig. 3, we clearly observed the vectorial basal-to-apical transport of pitavastatin across all of the double transfectants (OATP1B1/BCRP, OATP1B1/MDR1, and OATP1B1/MRP2) in contrast to that across the control and OATP1B1 single-transfected cells. The efflux transport clearance of pitavastatin normalized by the intracellular concentration did not differ much among MDR1, MRP2, and BCRP, the range being only 2-fold. In the case of pravastatin, we demonstrated previously that the efflux clearance of MRP2 was much higher than that of MDR1 and BCRP (Matsushima et al., 2005). Considering these facts, the relative contribution of MDR1 and BCRP to the biliary excretion of pitavastatin was larger than that of pravastatin. In the case of rats, the basal-to-apical flux of pitavastatin across the Oatp1b2/Mrp2 double transfectants was significantly higher than that across the Oatp1b2 single transfectants (Fig. 4). However, the ratio of basal-to-apical to apical-to-basal flux of pitavastatin in Oatp1b2/Mrp2 double-transfected cells divided by that in Oatp1b2 single-transfected cells was approximately 1.6, which was small in comparison with that of other substrates tested previously (Sasaki et al., 2004). Therefore, although pitavastatin is a substrate of rat Mrp2, the intrinsic efflux clearance of pitavastatin via rat Mrp2 seems to be relatively low.

The elimination of diflomotecan from plasma has been found to be delayed in patients with frequently observed SNP in BCRP (C421A/Q141K) (Sparreboom et al., 2004). Various reports suggested that this SNP affected the protein expression level of BCRP in the placenta without changing its intrinsic efflux clearance (Kondo et al., 2004; Kobayashi et al., 2005). On the other hand, both in vivo and in vitro studies revealed that the frequently observed haplotype OATP1B1*15 (N130D and V174A) reduced the nonrenal clearance of pravastatin (Nishizato et al., 2003; Iwai et al., 2004). We demonstrated previously that pitavastatin is taken up into hepatocytes mainly by OATP1B1 (Hirano et al., 2004). Taking these facts into consideration, further clinical studies are needed to investigate the effect of SNPs in OATP1B1 and BCRP on the pharmacokinetics of pitavastatin and to determine the importance of each transporter directly in humans.

In the present study, we have shown that pitavastatin is recognized by human and mouse BCRP in expression systems, and Bcrp is mainly involved in the biliary excretion of pitavastatin by knockout animals. BCRP can also accept other statins as a substrate, implying that it is important to

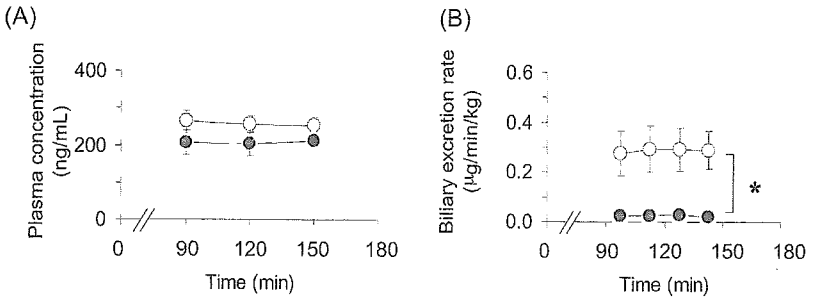

Fig. 6. Plasma concentration and biliary excretion rate of pitavastatin during constant intravenous infusion into wild-type and Bcrp1(−/−) mice. The plasma concentration (A) and biliary excretion rate (B) of pitavastatin were determined during constant intravenous infusion into wild-type (○) and Bcrp1(−/−) (●) mice. Each point plotted, with its vertical bar, represents the mean ± S.E. of four mice. *, $P < 0.05$

TABLE 3

Pharmacokinetic parameters of pitavastatin during constant intravenous infusion into wild-type and Bcrp1(−/−) mice

Data represent the mean ± S.E. (n = 4).

	$C_{ss,plasma}$	CL_{total}	$CL_{bile,plasma}$	$CL_{bile,liver}$	Liver Concentration	$K_{p,liver}$
	ng/ml	*ml/min/kg*	*ml/min/kg*	*ml/min/kg*	*ng/g*	
Wild type	254 ± 21	20.1 ± 1.8	1.21 ± 0.43	0.364 ± 0.032	813 ± 196	3.34 ± 1.03
Bcrp1(−/−)	213 ± 22	24.2 ± 2.5	0.110 ± 0.02*	0.0293 ± 0.0036**	798 ± 124	3.94 ± 0.83

* $P < 0.05$; ** $P < 0.01$.

$C_{ss,plasma}$, plasma steady-state concentration (mean of plasma concentration at 150 min); CL_{total}, total plasma clearance obtained by dividing the infusion rate by $C_{ss,plasma}$; $CL_{bile,plasma}$, biliary clearance normalized by the plasma concentration; $CL_{bile,liver}$, biliary clearance normalized by the liver concentration; $K_{p,liver}$, K_p value obtained by dividing the liver concentration by $C_{ss,plasma}$ (at 150 min).

estimate how the change of function and expression level of BCRP affects the pharmacokinetics of statins. In humans, because it is evident that pitavastatin is a substrate of BCRP, MDR1, and MRP2 by double transfectants, it will be important to estimate the contribution of each transporter to the biliary excretion of pitavastatin in humans.

Acknowledgments

We thank Dr. Alfred H Schinkel (The Netherlands Cancer Institute, the Netherlands) and Dr. Johan A Jonker (The Salk Institute for Biological Studies, San Diego, CA) for constructing Bcrp1(−/−) mice and giving us valuable comments, Dr. Piet Borst (The Netherlands Cancer Institute) for providing the MDCK II cells expressing MRP2 and MDR1, and Dr. Yoshihiro Miwa (University of Tsukuba, Tsukuba, Japan) for providing pEB6CAGMCS/SRZeo vector. We also thank Dr. Makoto Sasaki for constructing Oatp1b2/Mrp2 double-transfected cells and Chihiro Kondo for constructing human BCRP recombinant adenovirus. We also thank Sankyo Co., Ltd. (Tokyo, Japan) for providing radiolabeled pravastatin, Novartis Pharma K.K. (Basel, Switzerland) for providing radiolabeled fluvastatin, AstraZeneca PLC (London, UK), for providing radiolabeled rosuvastatin, and Kowa Co. Ltd. (Tokyo, Japan) for providing radiolabeled pitavastatin and unlabeled statins.

References

Adachi Y, Suzuki H, Schinkel AH, and Sugiyama Y (2004) Role of breast cancer resistance protein (Bcrp1/Abcg2) in the extrusion of glucuronide and sulfate conjugates from enterocytes to intestinal lumen. *Mol Pharmacol* **67:**923–928.

Allikmets R, Schriml LM, Hutchinson A, Romano-Spica V, and Dean M (1998) A human placenta-specific ATP-binding cassette gene (ABCP) on chromosome 4q22 that is involved in multidrug resistance. *Cancer Res* **58:**5337–5339.

Chandra P and Brouwer KL (2004) The complexities of hepatic drug transport: current knowledge and emerging concepts. *Pharm Res (NY)* **21:**719–735.

Cvetkovic M, Leake B, Fromm MF, Wilkinson GR, and Kim RB (1999) OATP and P-glycoprotein transporters mediate the cellular uptake and excretion of fexofenadine. *Drug Metab Dispos* **27:**866–871.

Doyle LA and Ross DD (2003) Multidrug resistance mediated by the breast cancer resistance protein BCRP (ABCG2). *Oncogene* **22:**7340–7358.

Fujino H, Saito T, Tsunenari Y, and Kojima J (2003) Interaction between several medicines and statins. *Arzneimittelforschung* **53:**145–153.

Fujino H, Yamada I, Shimada S, and Kojima J (2002) Metabolic fate of pitavastatin, a new inhibitor of HMG-CoA reductase-effect of cMOAT deficiency on hepatobiliary excretion in rats and of mdr1a/b gene disruption on tissue distribution in mice. *Drug Metab Pharmacokinet* **17:**449–456.

Garcia MJ, Reinoso RF, Sanchez Navarro A, and Prous JR (2003) Clinical pharmacokinetics of statins. *Methods Find Exp Clin Pharmacol* **25:**457–481.

Hirano M, Maeda K, Hayashi H, Kusuhara H, and Sugiyama Y (2005) Bile salt export pump (BSEP/ABCB11) can transport a nonbile acid substrate, pravastatin. *J Pharmacol Exp Ther* **314:**876–882.

Hirano M, Maeda K, Shitara Y, and Sugiyama Y (2004) Contribution of OATP2 (OATP1B1) and OATP8 (OATP1B3) to the hepatic uptake of pitavastatin in humans. *J Pharmacol Exp Ther* **311:**139–146.

Hirohashi T, Suzuki H, and Sugiyama Y (1999) Characterization of the transport properties of cloned rat multidrug resistance-associated protein 3 (MRP3). *J Biol Chem* **274:**15181–15185.

Imai Y, Nakane M, Kage K, Tsukahara S, Ishikawa E, Tsuruo T, Miki Y, and Sugimoto Y (2002) C421A polymorphism in the human breast cancer resistance protein gene is associated with low expression of Q141K protein and low-level drug resistance. *Mol Cancer Ther* **1:**611–616.

Iwai M, Suzuki H, Ieiri I, Otsubo K, and Sugiyama Y (2004) Functional analysis of single nucleotide polymorphisms of hepatic organic anion transporter OATP1B1 (OATP-C). *Pharmacogenetics* **14:**749–757.

Jonker JW, Buitelaar M, Wagenaar E, Van Der Valk MA, Scheffer GL, Scheper RJ, Plosch T, Kuipers F, Elferink RP, Rosing H, et al. (2002) The breast cancer resistance protein protects against a major chlorophyll-derived dietary phototoxin and protoporphyria. *Proc Natl Acad Sci USA* **99:**15649–15654.

Jonker JW, Smit JW, Brinkhuis RF, Maliepaard M, Beijnen JH, Schellens JH, and Schinkel AH (2000) Role of breast cancer resistance protein in the bioavailability and fetal penetration of topotecan. *J Natl Cancer Inst* **92:**1651–1656.

Kajinami K, Takekoshi N, and Saito Y (2003) Pitavastatin: efficacy and safety profiles of a novel synthetic HMG-CoA reductase inhibitor. *Cardiovasc Drug Rev* **21:**199–215.

Kimata H, Fujino H, Koide T, Yamada Y, Tsunenari Y, Yonemitsu M, and Yanagawa Y (1998) Studies on the metabolic fate of NK-104, a new inhibitor of HMG-CoA reductase: I. Absorption, distribution, metabolism and excretion in rats. *Xenobiol Metab Dispos* **13:**484–498.

Kobayashi D, Ieiri I, Hirota T, Takane H, Maegawa S, Kigawa J, Suzuki H, Nanba E, Oshimura M, Terakawa N, et al. (2005) Functional assessment of ABCG2 (BCRP) gene polymorphisms to protein expression in human placenta. *Drug Metab Dispos* **33:**94–101.

Kojima J, Ohshima T, Yoneda M, and Sawada H (2001) Effect of biliary excretion on the pharmacokinetics of pitavastatin (NK-104) in dogs. *Xenobio Metab Dispos* **16:**497–502.

Kondo C, Onuki R, Kusuhara H, Suzuki H, Suzuki M, Okudaira N, Kojima M, Ishiwata K, Jonker JW, and Sugiyama Y (2005) Lack of improvement of oral absorption of ME3277 by prodrug formation is ascribed to the intestinal efflux mediated by breast cancer resistant protein (BCRP/ABCG2). *Pharm Res (NY)* **22:**613–618.

Kondo C, Suzuki H, Itoda M, Ozawa S, Sawada J, Kobayashi D, Ieiri I, Mine K, Ohtsubo K, and Sugiyama Y (2004) Functional analysis of SNPs variants of BCRP/ABCG2. *Pharm Res (NY)* **21:**1895–1903.

Kruijtzer CM, Beijnen JH, Rosing H, ten Bokkel Huinink WW, Schot M, Jewell RC, Paul EM, and Schellens JH (2002) Increased oral bioavailability of topotecan in combination with the breast cancer resistance protein and P-glycoprotein inhibitor GF120918. *J Clin Oncol* **20:**2943–2950.

Maliepaard M, Scheffer GL, Faneyte IF, van Gastelen MA, Pijnenborg AC, Schinkel AH, van De Vijver MJ, Scheper RJ, and Schellens JH (2001) Subcellular localization and distribution of the breast cancer resistance protein transporter in normal human tissues. *Cancer Res* **61:**3458–3464.

Matsushima S, Maeda K, Kondo C, Hirano M, Sasaki M, Suzuki H, and Sugiyama Y (2005) Identification of the hepatic efflux transporters of organic anions using double-transfected Madin-Darby canine kidney II cells expressing human organic anion-transporting polypeptide 1B1 (OATP1B1)/multidrug resistance-associated protein 2, OATP1B1/multidrug resistance 1, and OATP1B1/breast cancer resistance protein. *J Pharmacol Exp Ther*, in press.

Merino G, Jonker JW, Wagenaar E, van Herwaarden AE, and Schinkel AH (2005a) The Breast Cancer Resistance Protein (BCRP/ABCG2) affects pharmacokinetics, hepatobiliary excretion and milk secretion of the antibiotic nitrofurantoin. *Mol Pharmacol* **65:**1758–1764.

Merino G, van Herwaarden AE, Wagenaar E, Jonker JW, and Schinkel AH (2005b) Sex-dependent expression and activity of the ABC transporter Breast Cancer Resistance Protein (BCRP/ABCG2) in liver. *Mol Pharmacol* **67:**1765–1771.

Mizuno N, Suzuki M, Kusuhara H, Suzuki H, Takeuchi K, Niwa T, Jonker JW, and Sugiyama Y (2004) Impaired renal excretion of 6-hydroxy-5,7-dimethyl-2-methylamino-4-(3-pyridylmethyl) benzothiazole (E3040) sulfate in breast cancer resistance protein (BCRP1/ABCG2) knockout mice. *Drug Metab Dispos* **32:**898–901.

Muller M, Meijer C, Zaman GJ, Borst P, Scheper RJ, Mulder NH, de Vries EG, and Jansen PL (1994) Overexpression of the gene encoding the multidrug resistance-associated protein results in increased ATP-dependent glutathione S-conjugate transport. *Proc Natl Acad Sci USA* **91:**13033–13037.

Nishizato Y, Ieiri I, Suzuki H, Kimura M, Kawabata K, Hirota T, Takane H, Irie S, Kusuhara H, Urasaki Y, et al. (2003) Polymorphisms of OATP-C (SLC21A6) and OAT3 (SLC22A8) genes: consequences for pravastatin pharmacokinetics. *Clin Pharmacol Ther* **73:**554–565.

Ogawa K, Suzuki H, Hirohashi T, Ishikawa T, Meier PJ, Hirose K, Akizawa T, Yoshioka M, and Sugiyama Y (2000) Characterization of inducible nature of MRP3 in rat liver. *Am J Physiol* **278:**G438–G446.

Sasaki M, Suzuki H, Aoki J, Ito K, Meier PJ, and Sugiyama Y (2004) Prediction of in vivo biliary clearance from the in vitro transcellular transport of organic anions across a double-transfected Madin-Darby canine kidney II monolayer expressing both rat organic anion transporting polypeptide 4 and multidrug resistance associated protein 2. *Mol Pharmacol* **66:**450–459.

Sasaki M, Suzuki H, Ito K, Abe T, and Sugiyama Y (2002) Transcellular transport of organic anions across a double-transfected Madin-Darby canine kidney II cell monolayer expressing both human organic anion-transporting polypeptide (OATP2/SLC21A6) and Multidrug resistance-associated protein 2 (MRP2/ABCC2). *J Biol Chem* **277:**6497–6503.

Sathirakul K, Suzuki H, Yasuda K, Hanano M, Tagaya O, Horie T, and Sugiyama Y (1993) Kinetic analysis of hepatobiliary transport of organic anions in Eisai hyperbilirubinemic mutant rats. *J Pharmacol Exp Ther* **265:**1301–1312.

Sparreboom A, Gelderblom H, Marsh S, Ahluwalia R, Obach R, Principe P, Twelves C, Verweij J, and McLeod HL (2004) Diflomotecan pharmacokinetics in relation to ABCG2 421C>A genotype. *Clin Pharmacol Ther* **76:**38–44.

Stein EA, Lane M, and Laskarzewski P (1998) Comparison of statins in hypertriglyceridemia *Am J Cardiol* **26;**81 66B–89B.

Suzuki M, Suzuki H, Sugimoto Y, and Sugiyama Y (2003) ABCG2 transports sulfated conjugates of steroids and xenobiotics. *J Biol Chem* **278:**22644–22649.

van Herwaarden AE, Jonker JW, Wagenaar E, Brinkhuis RF, Schellens JH, Beijnen JH, and Schinkel AH (2003) The breast cancer resistance protein (Bcrp1/Abcg2) restricts exposure to the dietary carcinogen 2-amino-1-methyl-6-phenylimidazo[4,5-b]pyridine. *Cancer Res* **63:**6447–6452.

Yamaoka K, Tanigawara Y, Nakagawa T, and Uno T (1981) A pharmacokinetic analysis program (multi) for microcomputer. *J Pharmacobiodyn* **4:**879–885.

Yamazaki M, Akiyama S, Ni'inuma K, Nishigaki R, and Sugiyama Y (1997) Biliary excretion of pravastatin in rats: contribution of the excretion pathway mediated by canalicular multispecific organic anion transporter. *Drug Metab Dispos* **25:**1123–1129.

Zamber CP, Lamba JK, Yasuda K, Farnum J, Thummel K, Schuetz JD, and Schuetz EG (2003) Natural allelic variants of breast cancer resistance protein (BCRP) and their relationship to BCRP expression in human intestine. *Pharmacogenetics* **13:**19–28.

Address correspondence to: Dr. Yuichi Sugiyama, Department of Molecular Pharmacokinetics, Graduate School of Pharmaceutical Sciences, The University of Tokyo, 7-3-1 Hongo, Bunkyo-ku, Tokyo, 113-0033 Japan. E-mail: sugiyama@mol.f.u-tokyo.ac.jp

Pharmaceutical Research, Vol. 22, No. 2, February 2005 (© 2005)
DOI: 10.1007/s01869-005-1869-8

Research Paper

Estimation of the Three-Dimensional Pharmacophore of Ligands for Rat Multidrug-Resistance–Associated Protein 2 Using Ligand-Based Drug Design Techniques

Shuichi Hirono,[1,3] Izumi Nakagome,[1] Rie Imai,[1] Kazuya Maeda,[2] Hiroyuki Kusuhara,[2] and Yuichi Sugiyama[2]

Received March 22, 2004; accepted July 19, 2004

Purpose. Multidrug-resistance–associated protein 2 (Mrp2) shows a broad substrate specificity toward amphiphilic organic anions. This study identified key functional groups of ligand molecules for binding to rat Mrp2, determined their relative locations, and examined substrate specificity through receptor mapping using three-dimensional (3D) quantitative structure-activity relationship (3D-QSAR) analysis.
Methods. Ligand-binding conformations were estimated using conformational analysis (CAMDAS) and molecular superposition (SUPERPOSE) methods to clarify the substrate specificity of rat Mrp2 in relation to 3D ligand structures.
Results. Two types of binding conformations of ligands for rat Mrp2 were identified. 3D-QSAR comparative molecular-field analysis (CoMFA) revealed a statistically significant model for one type, in which the steric, electrostatic, and log P contributions to the binding affinity for rat Mrp2 were 63.0%, 33.4%, and 3.6%, respectively ($n = 16$, $q^2 = 0.59$, $n = 3$, $r^2 = 0.99$, and $s = 0.08$).
Conclusions. The 3D pharmacophore of ligands for rat Mrp2, and the ligand-binding region of rat Mrp2, were estimated. Ligand recognition of rat Mrp2 is achieved through interactions in two hydrophobic and two electrostatically positive sites (primary binding sites). The broad substrate specificity of rat Mrp2 might result from the combination of secondary (two electrostatically positive and two electrostatically negative sites) and primary binding sites.

KEY WORDS: binding conformation; 3D pharmacophore; 3D-QSAR; rat Mrp2; substrate specificity.

INTRODUCTION

The liver is one of the most important organs in the detoxification of xenobiotics, and biliary excretion is a major pathway for their elimination. Compounds in the circulating blood are taken up by hepatocytes and are then metabolized and/or excreted into the bile. Many kinds of drugs and their metabolites are transported across the sinusoidal and bile canalicular membranes via carriers. The mechanism of transport across the bile canalicular membrane has been characterized using isolated canalicular membrane vesicles (CMVs), which revealed that several types of primary active transporters are responsible for ligand efflux from the hepatocytes into the bile. Among them, multidrug-resistance–associated protein-2 (Mrp2; gene symbol ABCC2) has an important role in the biliary excretion of many organic anions and glutathione or glucuronide conjugates (1–3).

Mrp2 is an ATP-binding cassette (ABC) transporter, which possesses two highly conserved ABC regions. The Eisai hyperbilirubinemic rat (EHBR), which has a hereditary Mrp2 deficiency owing to the insertion of a nonsense mutation (4), and the GY/TR$^-$ rat (5) have both helped to reveal the importance of Mrp2 in the biliary excretion of various types of organic anions. In the EHBR, the biliary excretion of Mrp2 substrates is drastically decreased, and the ATP-dependent uptake of Mrp2 substrates into CMVs prepared from EHBRs is greatly reduced compared with those prepared from normal rats.

These findings demonstrate that a wide range of organic anions can be substrates for Mrp2, which include: nonconjugated organic anions such as dibromosulfophthalein (6,7), cefodizime (β-lactam antibiotic) (7), pravastatin (a 3-hydroxy-3-methyl-glutaryl-coenzyme A reductase inhibitor) (8), temocaprilat (an angiotensin-converting enzyme inhibitor) (9), the carboxylate forms of CPT-11 and its active metabolite (SN-38, which is a topoisomerase inhibitor) (8), and a cyclic anionic peptide (BQ-123, which is an endothelin antagonist) (10); glutathione conjugates such as leukotriene C_4 (11) and DNP-SG (12); and glucuronide conjugates such as bilirubin glucuronide (13), E3040 glucuronide (14,15), and SN-38 glucuronide (16).

[1] School of Pharmaceutical Sciences, Kitasato University, Tokyo 108-8641, Japan.
[2] Graduate School of Pharmaceutical Sciences, University of Tokyo, Tokyo 113-0033, Japan.
[3] To whom correspondence should be addressed. (e-mail: hironos@pharm.kitasato-u.ac.jp)

ABBREVIATIONS: ABC, ATP-binding cassette; CAMDAS, Conformational Analyzer with Molecular Dynamics and Sampling; C log P, calculated log P; CMVs, canalicular membrane vesicles; CoMFA, comparative molecular-field analysis; EHBR, Eisai hyperbilirubinemic rat; MD, molecular dynamics; Mrp2, multidrug-resistance–associated protein 2; PLS, partial least squares; QSAR, quantitative structure-activity relationship; rmsd, root-mean-square deviation; SD, Sprague-Dawley.